US00RE49205E

(19) **United States**
(12) **Reissued Patent**
Johnson et al.

(10) **Patent Number: US RE49,205 E**
(45) **Date of Reissued Patent: Sep. 6, 2022**

(54) **JOHNSON LITHIUM OXYGEN ELECTROCHEMICAL ENGINE**

(71) Applicant: **Johnson IP Holding, LLC**, Atlanta, GA (US)

(72) Inventors: **Lonnie G. Johnson**, Atlanta, GA (US); **Tedric D. Campbell**, Lithia Springs, GA (US)

(73) Assignee: **JOHNSON IP HOLDING, LLC**, Atlanta, GA (US)

(21) Appl. No.: **16/437,141**

(22) Filed: **Jun. 11, 2019**

Related U.S. Patent Documents

Reissue of:
(64) Patent No.: **10,218,044**
Issued: **Feb. 26, 2019**
Appl. No.: **15/408,991**
Filed: **Jan. 18, 2017**

U.S. Applications:
(60) Provisional application No. 62/281,875, filed on Jan. 22, 2016.

(51) **Int. Cl.**
H01M 12/08 (2006.01)
H01M 8/04276 (2016.01)
(Continued)

(52) **U.S. Cl.**
CPC ***H01M 12/08*** (2013.01); ***H01M 4/134*** (2013.01); ***H01M 4/382*** (2013.01); ***H01M 4/8621*** (2013.01); ***H01M 8/04276*** (2013.01); ***H01M 10/0562*** (2013.01); ***H01M 10/0563*** (2013.01); ***H01M 10/399*** (2013.01); ***H01M 10/615*** (2015.04); ***H01M 10/617*** (2015.04); ***H01M 10/63*** (2015.04); ***H01M 10/652*** (2015.04); ***H01M 10/654*** (2015.04);
(Continued)

(58) **Field of Classification Search**
None
See application file for complete search history.

(56) **References Cited**

U.S. PATENT DOCUMENTS

3,237,078 A 2/1966 Mallory
3,393,355 A 7/1968 Whoriskey et al.
(Continued)

FOREIGN PATENT DOCUMENTS

CN 1866583 A 11/2006
CN 101434417 A 5/2009
(Continued)

OTHER PUBLICATIONS

Office Action dated Dec. 17, 2020 in CN Application No. 201780007783.8.
(Continued)

Primary Examiner — Sean E Vincent
(74) *Attorney, Agent, or Firm* — Panitch Schwarze Belisario & Nadel LLP

(57) **ABSTRACT**

A rechargeable lithium air battery is provided. The battery contains a ceramic separator forming an anode chamber, a molten lithium anode contained in the anode chamber, an air cathode, and a non-aqueous electrolyte. The cathode has a temperature gradient comprising a low temperature region and a high temperature region, and the temperature gradient provides a flow system for reaction product produced by the battery.

41 Claims, 8 Drawing Sheets

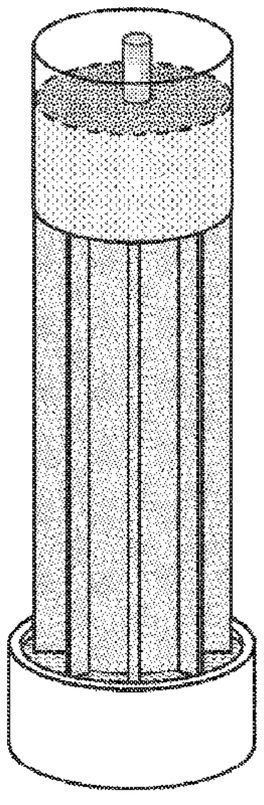

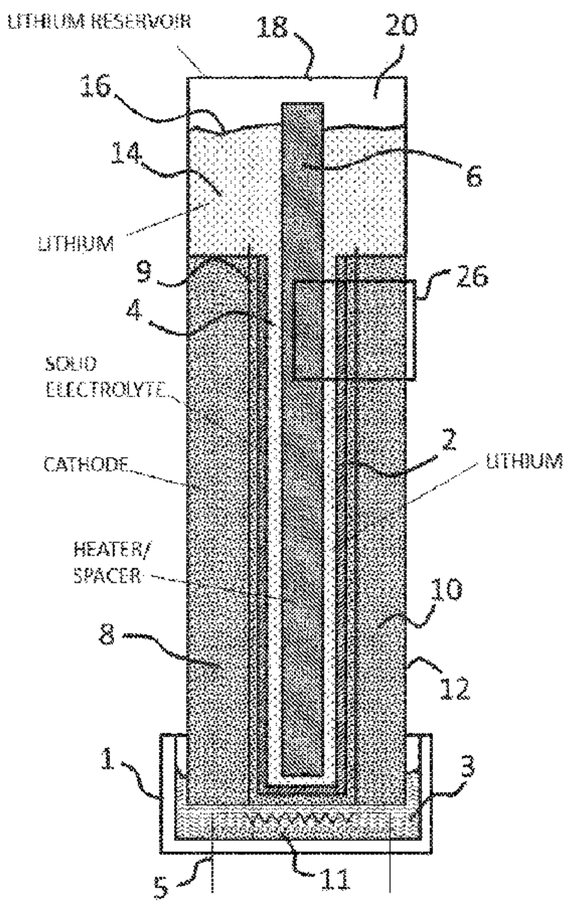

(51) **Int. Cl.**

H01M 12/02	(2006.01)
H01M 10/652	(2014.01)
H01M 10/617	(2014.01)
H01M 10/654	(2014.01)
H01M 4/86	(2006.01)
H01M 10/615	(2014.01)
H01M 4/38	(2006.01)
H01M 10/655	(2014.01)
H01M 10/0569	(2010.01)
H01M 10/48	(2006.01)
H01M 50/431	(2021.01)
H01M 50/434	(2021.01)
H01M 50/437	(2021.01)
H01M 10/6551	(2014.01)
H01M 10/6571	(2014.01)
H01M 10/39	(2006.01)
H01M 10/0562	(2010.01)
H01M 4/134	(2010.01)
H01M 10/63	(2014.01)
H01M 10/0563	(2010.01)
H01M 4/02	(2006.01)

(52) **U.S. Cl.**

CPC ***H01M 10/655*** (2015.04); ***H01M 10/6551*** (2015.04); ***H01M 10/6571*** (2015.04); ***H01M 12/02*** (2013.01); ***H01M 50/431*** (2021.01); ***H01M 50/434*** (2021.01); ***H01M 50/437*** (2021.01); *H01M 10/0569* (2013.01); *H01M 10/486* (2013.01); *H01M 2004/027* (2013.01); *H01M 2004/8689* (2013.01); *H01M 2300/0048* (2013.01); *H01M 2300/0068* (2013.01); *Y02E 60/10* (2013.01); *Y02E 60/50* (2013.01)

(56) **References Cited**

U.S. PATENT DOCUMENTS

4,299,682	A	11/1981	Oda et al.
4,303,877	A	12/1981	Meinhold
4,352,068	A	9/1982	Weppner
4,386,020	A	5/1983	Hartwig et al.
4,419,421	A	12/1983	Wichelhaus et al.
4,495,078	A	1/1985	Bell et al.
4,513,069	A	4/1985	Kreuer et al.
4,526,855	A	7/1985	Hartwig et al.
4,614,905	A	9/1986	Petersson et al.
4,654,281	A	3/1987	Anderman et al.
4,704,341	A	11/1987	Weppner et al.
4,710,848	A	12/1987	Schlechtriemen et al.
4,719,401	A	1/1988	Altmejd
4,728,590	A	3/1988	Redey
4,777,119	A	10/1988	Brault et al.
4,792,752	A	12/1988	Schlechtriemen et al.
4,803,134	A	2/1989	Sammells
4,885,267	A	12/1989	Takahara et al.
4,931,214	A	6/1990	Worrell et al.
5,023,153	A	6/1991	Weppner
5,202,788	A	4/1993	Weppner
5,238,761	A	8/1993	Ryan
5,260,821	A	11/1993	Chu et al.
5,270,635	A	12/1993	Hoffman et al.
5,291,116	A	3/1994	Feldstein
5,314,765	A	5/1994	Bates
5,322,601	A	6/1994	Liu et al.
5,336,573	A	8/1994	Zuckerbrod et al.
5,338,625	A	8/1994	Bates et al.
5,362,581	A	11/1994	Chang et al.
5,387,857	A	2/1995	Honda et al.
5,411,592	A	5/1995	Ovshinsky et al.
5,432,026	A	7/1995	Sahm et al.
5,445,906	A	8/1995	Hobson et al.
5,455,126	A	10/1995	Bates et al.
5,474,959	A	12/1995	Schafer et al.
5,512,147	A	4/1996	Bates et al.
5,522,955	A	6/1996	Brodd
5,561,004	A	10/1996	Bates et al.
5,567,210	A	10/1996	Bates et al.
5,569,520	A	10/1996	Bates
5,597,660	A	1/1997	Bates et al.
5,612,152	A	3/1997	Bates
5,654,084	A	8/1997	Egert
5,677,081	A	10/1997	Iwamoto et al.
5,705,293	A	1/1998	Hobson
5,778,515	A	7/1998	Menon
5,783,333	A	7/1998	Mayer
5,783,928	A	7/1998	Okamura
5,811,205	A	9/1998	Andrieu et al.
5,821,733	A	10/1998	Turnbull
6,022,642	A	2/2000	Tsukamoto et al.
6,136,472	A	10/2000	Barker et al.
6,139,986	A	10/2000	Kurokawa et al.
6,168,884	B1	1/2001	Neudecker et al.
6,182,340	B1	2/2001	Bishop
6,201,123	B1	3/2001	Daikai et al.
6,242,129	B1	6/2001	Johnson
6,255,122	B1	7/2001	Duncombe et al.
6,387,563	B1	5/2002	Bates
6,413,285	B1	7/2002	Chu et al.
6,413,672	B1	7/2002	Suzuki et al.
6,541,161	B1	4/2003	Scanlon, Jr.
6,679,926	B1	1/2004	Kajiura et al.
6,827,921	B1	12/2004	Singhal et al.
6,852,139	B2	2/2005	Zhang et al.
6,886,240	B2	5/2005	Zhang et al.
6,887,612	B2	5/2005	Bitterlich et al.
7,230,404	B2	6/2007	Kimoto et al.
7,276,308	B2	10/2007	Formanski et al.
7,510,800	B2	3/2009	Yoshida et al.
7,524,580	B1	4/2009	Birke et al.
7,540,886	B2	6/2009	Zhang et al.
7,557,055	B2	7/2009	Zhang et al.
7,674,559	B2	3/2010	Min et al.
7,691,536	B2	4/2010	Johnson
7,732,096	B2	6/2010	Thackeray et al.
7,776,478	B2	8/2010	Klaassen
7,824,795	B2	11/2010	Yoshida et al.
7,901,658	B2	3/2011	Weppner et al.
7,914,932	B2	3/2011	Yoshida et al.
7,998,622	B2	8/2011	Inda
8,092,941	B2	1/2012	Weppner et al.
8,173,292	B2	5/2012	Kato
8,192,869	B2	6/2012	Teramoto
8,211,496	B2	7/2012	Johnson et al.
8,221,916	B2	7/2012	Inda
8,313,721	B2	11/2012	Thackeray et al.
8,383,268	B2	2/2013	Inda
8,431,287	B2	4/2013	Teramoto
8,476,174	B2	7/2013	Inda
8,568,921	B1	10/2013	Johnson
8,778,546	B2	7/2014	Farmer
8,795,868	B1	8/2014	Miles
8,808,407	B2	8/2014	Inda
8,822,077	B2	9/2014	Katoh
8,852,816	B2	10/2014	Ogasa
8,883,355	B2	11/2014	Inda
8,951,681	B2	2/2015	Katoh
9,034,525	B2	5/2015	Babic et al.
9,153,838	B2	10/2015	Ogasa
9,159,989	B2	10/2015	Ogasa
9,178,255	B2	11/2015	Kumar et al.
9,203,123	B2	12/2015	Prochazka, Jr. et al.
9,263,770	B2	2/2016	Boxley et al.
9,266,780	B2	2/2016	Ogasa
9,379,375	B2	6/2016	Sugiura et al.
9,385,405	B2	7/2016	Murata et al.
9,413,033	B2	8/2016	Ogasa
9,413,036	B2	8/2016	Bhavaraju et al.
9,425,454	B2	8/2016	Sugiura et al.
9,450,278	B2	9/2016	Kim et al.
9,680,191	B2	6/2017	Lee et al.
9,711,822	B2	7/2017	Nakashima et al.

(56) **References Cited**

U.S. PATENT DOCUMENTS

9,917,304	B2	3/2018	Lee et al.	
9,954,260	B2	4/2018	Ho	
9,997,813	B2	6/2018	Park et al.	
10,566,611	B2	2/2020	Allie et al.	
10,686,224	B2	6/2020	Angell et al.	
10,693,170	B2	6/2020	Jin et al.	
10,734,686	B2	8/2020	Robins et al.	
10,797,340	B2	10/2020	Lee et al.	
2001/0014505	A1	8/2001	Duncombe et al.	
2001/0036578	A1	11/2001	Nishida et al.	
2002/0000541	A1	1/2002	Sasaki et al.	
2002/0008706	A1	4/2002	Mayes et al.	
2002/0119375	A1	8/2002	Zhang	
2003/0012996	A1	1/2003	Bitterlich et al.	
2003/0030039	A1	2/2003	Sasaki et al.	
2003/0118897	A1	6/2003	Mino et al.	
2003/0157407	A1	8/2003	Kosuzu et al.	
2004/0081888	A1	4/2004	Thackeray et al.	
2004/0101761	A1	5/2004	Park et al.	
2004/0111874	A1	6/2004	Schierle-Arndt et al.	
2004/0118700	A1	6/2004	Schierle-Arndt et al.	
2004/0151986	A1	8/2004	Park et al.	
2004/0191617	A1	9/2004	Visco et al.	
2005/0084758	A1	4/2005	Yamamoto et al.	
2005/0095506	A1	5/2005	Klaassen	
2005/0100793	A1	5/2005	Jonghe et al.	
2005/0147890	A1	7/2005	Shembel et al.	
2005/0266150	A1	12/2005	Yong et al.	
2006/0046149	A1	3/2006	Yong et al.	
2006/0068282	A1	3/2006	Kishi et al.	
2006/0093916	A1	5/2006	Howard et al.	
2006/0165578	A1	7/2006	Sasaki et al.	
2006/0246355	A1	11/2006	Min et al.	
2006/0287188	A1	12/2006	Borland et al.	
2007/0031323	A1	2/2007	Baik et al.	
2007/0048617	A1	3/2007	Inda	
2007/0087269	A1	4/2007	Inda	
2007/0148545	A1	6/2007	Amine et al.	
2007/0148553	A1	6/2007	Weppner	
2007/0231704	A1	10/2007	Inda	
2007/0264579	A1	11/2007	Ota	
2008/0131781	A1	6/2008	Yong et al.	
2008/0220334	A1	9/2008	Inda	
2008/0241698	A1	10/2008	Katoh	
2008/0268346	A1	10/2008	Inda	
2009/0004371	A1	1/2009	Johnson et al.	
2009/0068563	A1	3/2009	Kanda et al.	
2009/0081554	A1	3/2009	Takada et al.	
2009/0081555	A1	3/2009	Teramoto	
2009/0092903	A1	4/2009	Johnson et al.	
2009/0098281	A1	4/2009	Zhang et al.	
2009/0142669	A1	6/2009	Shinohara et al.	
2009/0162755	A1	6/2009	Neudecker	
2009/0194222	A1	8/2009	Teramoto	
2009/0197178	A1	8/2009	Inda	
2009/0197182	A1	8/2009	Katoh	
2009/0214957	A1	8/2009	Okada et al.	
2009/0274832	A1	11/2009	Inda	
2010/0028782	A1	2/2010	Inda	
2010/0047696	A1	2/2010	Yoshida et al.	
2010/0104948	A1	4/2010	Skotheim et al.	
2010/0203383	A1	8/2010	Weppner	
2010/0291443	A1	11/2010	Farmer	
2010/0308278	A1	12/2010	Kepler et al.	
2011/0053001	A1	3/2011	Babic et al.	
2011/0059369	A1	3/2011	Nan et al.	
2011/0076542	A1	3/2011	Farmer	
2011/0086274	A1	4/2011	Chang et al.	
2011/0133136	A1	6/2011	Weppner et al.	
2011/0177397	A1	7/2011	Ogasa	
2011/0209859	A1	9/2011	Reinke et al.	
2011/0223460	A1	9/2011	Farmer	
2011/0223467	A1	9/2011	Shacklette et al.	
2011/0223487	A1	9/2011	Johnson et al.	
2011/0300451	A1	12/2011	Inda	
2011/0318650	A1	12/2011	Zhang et al.	
2012/0100433	A1	4/2012	Suyama et al.	
2012/0141881	A1	6/2012	Geier et al.	
2012/0196189	A1	8/2012	Babic et al.	
2012/0237834	A1	9/2012	Ogasa	
2012/0251882	A1	10/2012	Moon et al.	
2012/0264021	A1	10/2012	Sugiura et al.	
2012/0270115	A1	10/2012	Johnson	
2013/0011751	A1	1/2013	Nakada et al.	
2013/0011752	A1	1/2013	Tanaami et al.	
2013/0017454	A1	1/2013	Sato et al.	
2013/0095394	A1	4/2013	Tanaami et al.	
2013/0157149	A1*	6/2013	Peled	H01M 4/38 429/405
2013/0164616	A1	6/2013	Nakada et al.	
2013/0230777	A1	9/2013	Babic et al.	
2013/0273437	A1	10/2013	Yoshioka et al.	
2013/0309551	A1	11/2013	Ogasa	
2013/0344416	A1	12/2013	Sakamoto et al.	
2014/0008006	A1	1/2014	Lee et al.	
2014/0011080	A1	1/2014	Lee et al.	
2014/0011095	A1	1/2014	Lee et al.	
2014/0023933	A1	1/2014	Chiga et al.	
2014/0038058	A1	2/2014	Holzapfel et al.	
2014/0065456	A1*	3/2014	Bhavaraju	H01M 10/36 429/81
2014/0099538	A1	4/2014	Johnson et al.	
2014/0099556	A1	4/2014	Johnson et al.	
2014/0287305	A1	9/2014	Wachsman et al.	
2015/0037688	A1	2/2015	Otsuka et al.	
2015/0056518	A1	2/2015	Babic et al.	
2015/0056520	A1	2/2015	Thokchom et al.	
2015/0099187	A1	4/2015	Cui et al.	
2015/0099197	A1	4/2015	Nakashima et al.	
2015/0333307	A1	11/2015	Thokchom et al.	
2016/0028133	A1	1/2016	Miles	
2016/0036109	A1	2/2016	Kim et al.	
2016/0149261	A1	5/2016	Zaghib et al.	
2016/0164153	A1	6/2016	Kim et al.	
2016/0181657	A1	6/2016	Kawaji et al.	
2016/0329539	A1	11/2016	Kawaji et al.	
2016/0336583	A1	11/2016	Smith et al.	
2017/0179521	A1*	6/2017	Sakamoto	H01M 10/0562
2017/0214106	A1	7/2017	Johnson et al.	
2017/0222287	A1	8/2017	Suzuki et al.	
2019/0296276	A1	9/2019	Bradwell et al.	
2019/0372148	A1	12/2019	He et al.	
2021/0218091	A1	7/2021	Uddin et al.	
2021/0265616	A1	8/2021	Kim et al.	

FOREIGN PATENT DOCUMENTS

CN	101494299	A	7/2009
CN	102214827	A	10/2011
CN	102013536	B	10/2012
CN	102934279	A	2/2013
CN	104245624	A	12/2014
CN	206048735	U	3/2017
CN	107437636	A	12/2017
CN	206921981	U	1/2018
CN	207413450	U	5/2018
DE	4309070	A1	9/1994
DE	102004010892	B3	11/2005
DE	102007030604	A1	1/2009
DE	102010019187	A1	11/2011
DE	102015220354	A1	4/2017
EP	0070020	A1	1/1983
EP	0033935	B1	8/1985
EP	0177062	A2	4/1986
EP	0190605	A2	8/1986
EP	0206339	A2	12/1986
EP	0226955	A2	7/1987
EP	0232513	A2	8/1987
EP	0243975	A2	11/1987
EP	0249802	A2	12/1987
EP	238383	B1	8/1989
EP	0408039	A2	1/1991
EP	0227996	B1	7/1991
EP	0470597	A2	2/1992

(56) **References Cited**

FOREIGN PATENT DOCUMENTS

EP	0693581	B1	5/1998
EP	1271683	A2	1/2003
EP	1431422	A1	6/2004
EP	1431423	A1	6/2004
EP	1237212	A3	4/2005
EP	2037527	A1	3/2009
EP	2086040	A2	8/2009
EP	2181971	A1	5/2010
EP	2685551	A1	1/2014
EP	2706598	A1	3/2014
EP	2903060	A1	8/2015
FR	2466107	A1	3/1981
GB	1329688	A	9/1973
GB	1599792	A	10/1981
GB	2226441	B	12/1992
JP	S628452	A	1/1987
JP	H05-310417	A	11/1993
JP	H07235291	A	9/1995
JP	2000311710	A	11/2000
JP	2000331680	A	11/2000
JP	2000331684	A	11/2000
JP	2001126757	A	5/2001
JP	2001126758	A	5/2001
JP	2001243954	A	9/2001
JP	2003132921	A	5/2003
JP	2004127613	A	4/2004
JP	2006260887	A	9/2006
JP	2006261008	A	9/2006
JP	2006310295	A	11/2006
JP	2008505458	A	2/2008
JP	2009176741	A	8/2009
JP	2010067499	A	3/2010
JP	2010080426	A	4/2010
JP	2010129190	A	6/2010
JP	2010132533	A	6/2010
JP	2010244729	A	10/2010
JP	2011134675	A	7/2011
JP	2011150817	A	8/2011
JP	2011249254	A	12/2011
JP	2012003940	A	1/2012
JP	2012099315	A	5/2012
JP	2012146479	A	8/2012
JP	2013037992	A	2/2013
JP	2013157084	A	8/2013
JP	2013532359	A	8/2013
JP	2015013775	A	1/2015
JP	2015138741	A	7/2015
JP	2015144061	A	8/2015
JP	2015204215	A	11/2015
JP	2015230801	A	12/2015
KR	20140006046	A	1/2014
RU	2126192	C1	2/1999
WO	2005085138	A1	9/2005
WO	2006005066	A2	1/2006
WO	2006019245	A1	2/2006
WO	2007004590	A1	1/2007
WO	2007075867	A2	7/2007
WO	2009003695	A2	1/2009
WO	2009029746	A1	3/2009
WO	2011007445	A1	1/2011
WO	2011125481	A1	10/2011
WO	2011150528	A1	12/2011
WO	2011154869	A2	12/2011
WO	2011156392	A1	12/2011
WO	2012008422	A1	1/2012
WO	2012016606	A1	2/2012
WO	2012018831	A1	2/2012
WO	2012128374	A1	9/2012
WO	2012144553	A1	10/2012
WO	2013049460	A1	4/2013
WO	2013085557	A1	6/2013
WO	2013130983	A2	9/2013
WO	2013131005	A2	9/2013
WO	2014058683	A1	4/2014
WO	2014058684	A2	4/2014
WO	2015007680	A1	1/2015
WO	2015104538	A1	7/2015
WO	2015128982	A1	9/2015
WO	2015151144	A1	10/2015
WO	2016102373	A1	6/2016
WO	2016116400	A1	7/2016
WO	2016141765	A1	9/2016
WO	2020225313	A1	11/2020

OTHER PUBLICATIONS

Extended European Search Report dated Feb. 12, 2020 in EP Application No. 19192837.3.

Kim et al., "A review of lithium and non-lithium based solid state batteries," Journal of Power Sources, vol. 282, pp. 299-322 (2015).

Office Action dated Jun. 7, 2018 in U.S. Appl. No. 15/408,991, by Johnson.

Office Action dated Jun. 10, 2019 in JP Application No. 2018538203 (Partial English Translation).

"All-Solid-State Lithium-Ion Battery Using Li2.2C0.8B0 203 Electrolyte" External Program 20th Century International Conferencer, Presented on Poster Board, 2 pgs (Jun. 15, 2015).

Aaltonen et al., "Lithium Lanthanum Titanate Thin Films Grown by Atomic Layer Deposition for All-Solid-State Lithium Ion Battery Applications," Abstract #688, The 15th International Meeting on Lithium Batteries (2010).

Adachi et al., "Ionic Conducting Lanthanide Oxides," Chem. Rev., vol. 102, pp. 2405-2429 (2002).

Ahn et al., "Characteristics of Amorphous Lithium Lanthanum Titanate Electrolyte Thin Films Grown by PLD for Use in Rechargeable Lithium Microbatteries," Electrochemical and Solid-State Letters, vol. 8, No. 2, pp. A75-A78 (2005).

Ahn et al., "Characteristics of Perovskite (Li0.5La0.5)TiO3 Solid Electrolyte Thin Films Grown by Pulsed Laser Deposition for Rechargeable Lithium Microbattery," Electrochimica Acta, vol. 50, pp. 371-374 (2004).

Ahn et al., "Effect of Li0.5La0.5TiO3 Solid Electrolyte Films on Electrochemical Properties of LiCoO2 Thin Film Cathodes with Different Rapid-Thermal Annealing Conditions," Journal of Vacuum Science & Technology B, vol. 23, No. 5, pp. 2089-2094 (2005).

Allen et al., "Effect of substitution (Ta, Al, Ga) on the conductivity of Li7La3Zr2012," Journal of Power Sources, vol. 206, pp. 315-319(2012).

Allnatt et al., "Atomic Transport in Solids," Cambridge University Press, pp. ix-xiii (2003).

Annamareddy et al., "Ion Hopping and Constrained Li Diffusion Pathways in the Superionic State of Antifluorite Li2O," Entropy, vol. 19, No. 227, pp. 1-11 (2017).

Aruna et al., "Combustion Synthesis and Nanomaterials," Current Opinion in Solid State and Materials Science, vol. 12, pp. 44-50 (2008).

Awaka et al., "Synthesis and Structure Analysis of Tetragonal Li7La3Zr2012 with the Garnet-Related Type Structure," Journal of Solid State Chemistry, vol. 182, No. 8, pp. 2046-2052 (2009).

Balkanski et al., "Integrable lithium solid-state microbatteries," Journal of Power Sources, vol. 26, pp. 615-622 (1989).

Bates et al., "Rechargeable Thin-Film Lithium Batteries," Oak Ridge National Laboratory Publication, 9 pgs (1993).

Billinge, "The Nanostructure Problem," Physics, vol. 3, No. 25, pp. 1-3 (2010).

Birke et al., "A first approach to a monolithic all solid state inorganic lithium battery," Solid State Ionics, vol. 118, pp. 149-157 (1999).

Birke et al., "Electrolytic Stability Limit and Rapid Lithium Insertion in the Fast-Ion-Conducting Li0.29La0.57TiO3 Perovskite-Type Compound," Journal of the Electrochemical Society, vol. 144, No. 6, pp. L167-L169 (1997).

Bohnke et al., "Mechanism of Ionic Conduction and Electrochemical Intercalation of Lithium into the Perovskite Lanthanum Lithium Titanate," Solid State Ionics, vol. 91, pp. 21-31 (1996).

Boyd, "Thin Film Growth by Pulsed Laser Deposition," Ceramics International, vol. 22, pp. 429-434 (1996).

Boyle et al., "All-Ceramic Thin Film Battery," Sandia Report 2002-3615 Unlimited Release, 53 pages (Nov. 2002).

(56) **References Cited**

OTHER PUBLICATIONS

Brenier, "Stress and Moisture-Sorption in Ozone-Annealed Films of Zirconium Oxide Obtained from Sol-Gel," Journal of Sol-Gel Science and Technology, vol. 25, pp. 57-63 (2002).
Brinker et al., "Sol-Gel Science: The Physics and Chemistry of Sol-Gel Processing," Academic Press, pp. 21, 95, 153, 513, 675, 742, 787, and 837 (1990).
Buschmann et al., "Structure and dynamics of the fast lithium ion conductor 'Li7La3Zr2012," Physical Chemistry Chemical Physics, vol. 13, p. 19378-19392 (2011) (Abstract Only).
Cao et al., "Microstructure and Ionic Conductivity of Sb-doped Li7La3Zr2012," Journal of Inorganic Materials,vol. 29, No. 2, pp. 220-224 (2014).
Chabal et al., "Safer High-performance Electrodes, Solid Electrolytes, and Interface Reactions for Lithium-Ion Batteries," Material Matters, vol. 8, No. 4, pp. 104-110 (2013).
Chen et al., "High Capacity and Cyclic Performance in a Three-Dimensional Composite Electrode Filled with Inorganic Solid Electrolyte," Journal of Power Sources, vol. 249, pp. 306-310 (2014).
Chen et al., "Improving ionic conductivity of Li0.35La0.55Ti03 ceramics by introducing Li7La3Zr2012 sol into the precursor powder," Solid State Ionics, vol. 235, pp. 8-13 (2013).
Cussen, "Structure and Ionic Conductivity in Lithium Garnets," Journal of Materials Chemistry, vol. 20, pp. 5167-5173 (2010).
Davison et al., "Low Cost, Novel Methods for Fabricating All-Solid-State Lithium Ion Batteries," downloaded from web page: <http://www.wpi.edu/Pubs/E-project/Available/E-project-042312-141301/unrestricted/SS_Lithium_Ion_Battery_MQP_Final_Report.pdf>, Download date: Apr. 23, 2012, original posting date unknown, 126 pages.
Decision to Grant dated Nov. 24, 2020 in KR Application No. 1020187020835.
Drabold, "Topics in the Theory of Amorphous Materials," The European Physical Journal B, vol. 68, pp. 1-21 (2009).
Elliott, "Physics of Amorphous Materials," Longman Scientific & Technical, Ed. 2, pp. v-vi (1990).
Examination Report dated Jun. 22, 2016 in EP Application No. 13776685.3.
Examination Report dated Nov. 30, 2016 in EP Application No. 13776685.3.
Extended European Search Report dated Feb. 8, 2017 in EP Application 16202541.
Extended European Search Report dated Mar. 16, 2017 in EP Application No. 17150717.
Furusawa et al., "Ionic Conductivity of Amorphous Lithium Lanthanum Titanate Thin Film," Solid State Ionics, vol. 176, pp. 553-558 (2005).
Gao et al., "Sol-gel Synthesis and Electrical Properties of Li5La3Ta2O12 Lithium Ionic Conductors," Solid State Ionics, vol. 181, Nos. 1-2, pp. 33-36 (2009).
Geiger et al., "Crystal Chemistry and Stability of'Li7La3Zr2O12' Garnet: A Fast Lithium-Ion Conductor," Inorganic Chemistry, vol. 50, pp. 1089-1097 (2011).
Giordani et al., "A Molten Salt Lithium-Oxygen Battery," Journal of the American Chemical Society, 26 pages (2016).
Glass et al., "Ionic Conductivity of Quenched Alkali Niobate and Tantalate Glasses," Journal of Applied Physics, vol. 19, No. 9, pp. 4808-4811 (1978).
Goodenough et al., "Challenges for Rechargeable Li Batteries," Chemistry of Materials, vol. 22, No. 3, pp. 587-603 (2010).
Hámáláinen et al., "Lithium Phosphate Thin Films Grown by Atomic Layer Deposition," Journal of The Electrochemical Society, vol. 15 9, No. 3, pp. A259-A263 (2012).
Huggins, "Advanced Batteries: Materials Science Aspects," Springer, Ed. 1, p. xvii-xxx and pp. 368-371 (2008).
Inaguma et al., "High Ionic Conductivity in Lithium Lanthanum Titanate," Solid State Communications, vol. 86, No. 10, pp. 689-693 (1993).
Int'l Preliminary Examination Report on Patentability dated Jul. 5, 2018 in Int'l Application No. PCT/US2016/068105.
Int'l Preliminary Report on Patentability dated Feb. 14, 2013 in Int'l Application No. PCT/US2011/046289.
Int'l Preliminary Report on Patentability dated Apr. 23, 2015 in Int'l Application No. PCT/US2013/063160.
Int'l Preliminary Report on Patentability dated Sep. 2, 2014 in Int'l Application No. PCT/US2013/028672.
Int'l Preliminary Report on Patentability dated Sep. 12, 2014 in Int'l Application No. PCT/US2013/028633.
Extended European Search Report dated Dec. 16, 2021 in EP Application No. 21186896.3.
Office Action dated Feb. 9, 2022 in EP Application No. 16823507.5.
Office Action dated Jan. 22, 2016 in EP Application No. 13776685.3.
Office Action dated Jan. 24, 2012 in U.S. Appl. No. 12/198,421 by Johnson.
Office Action dated Jan. 25, 2018 in CN Application No. 201380052598.2.
Office Action dated Jan. 31, 2019 in U.S. Appl. No. 15/387,143, by Allie.
Office Action dated Feb. 7, 2018 in U.S. Appl. No. 14/382,194, by Thokchom.
Office Action dated Feb. 10, 2016 in U.S. Appl. No. 13/829,525 by Johnson.
Office Action dated Feb. 15, 2017 in CN Application No. 201380052598.2.
Office Action dated Feb. 20, 2017 in JP Application No. 2014-560097.
Office Action dated Feb. 21, 2020 in KR Application No. 1020187020835.
Office Action dated Mar. 2, 2016 in CN Application No. 201380023413.5.
Office Action dated Mar. 14, 2018 in U.S. Appl. No. 13/829,525, by Johnson.
Office Action dated Mar. 17, 2020 in U.S. Appl. No. 16/109,295, by Johnson.
Office Action dated Mar. 26, 2021 in CN Application No. 201680075318.3.
Office Action dated Mar. 30, 2018 in CN Application No. 201380023413.5.
Office Action dated Apr. 9, 2015 in U.S. Appl. No. 13/829,525 by Johnson.
Office Action dated Apr. 10, 2018 in EP Application No. 16202541.5.
Office Action dated Apr. 29, 2014 in U.S. Appl. No. 12/848,991 by Babic.
Office Action dated May 1, 2014 in U.S. Appl. No. 13/410,895, by Babic.
Office Action dated May 4, 2015 in U.S. Appl. No. 13/829,951 by Johnson.
Office Action dated May 4, 2016 in KR Application No. 10-2014-7027734.
Office Action dated May 19, 2017 in U.S. Appl. No. 12/198,421, by Johnson.
Office Action dated May 30, 2017 in JP Application No. 2015-535772.
Office Action dated Jun. 2, 2016 in CN Application No. 201380052598.2.
Office Action dated Jun. 5, 2019 in CN Application No. 201380052598.2.
Office Action dated Jun. 12, 2017 in U.S. Appl. No. 14/382,194, by Thokchom.
Office Action dated Jun. 13, 2017 in JP Application No. 2015-535773.
Office Action dated Jun. 15, 2017 in U.S. Appl. No. 14/382,191, by Thokchom.
Office Action dated Jun. 17, 2019 in U.S. Appl. No. 15/387,143, by Allie.
Office Action dated Jun. 19, 2014 in U.S. Appl. No. 13/829,951, by Johnson.
Office Action dated Jun. 24, 2019 in JP Application No. 2018551909.
Office Action datedJun. 26, 2015 in U.S. Appl. No. 14/530,171 by Babic.

(56) **References Cited**

OTHER PUBLICATIONS

Office Action dated Jun. 29, 2018 in U.S. Appl. No. 14/382,194, by Thokchom.
Office Action dated Jul. 1, 2015 in U.S. Appl. No. 13/829,525 by Johnson.
Office Action dated Jul. 5, 2016 in CN Application No. 201380052635.X.
Office Action dated Jul. 13, 2011 in U.S. Appl. No. 12/163,044, by Johnson.
Office Action dated Jul. 15, 2016 in KR Application No. 10-2014-7027734.
Office Action dated Jul. 20, 2017 in CN Application No. 201380052635.X.
Office Action dated Jul. 21, 2016 in U.S. Appl. No. 13/829,951, by Johnson.
Office Action dated Jul. 27, 2016 in U.S. Appl. No. 13/829,525, by Johnson.
Office Action dated Aug. 3, 2020 in CN Application No. 201680075318.3.
Office Action dated Aug. 7, 2017 in U.S. Appl. No. 13/829,525, by Johnson.
Office Action dated Aug. 7, 2019 in U.S. Appl. No. 12/198,421, by Johnson.
Office Action dated Aug. 9, 2021 in U.S. Appl. No. 12/198,421, by Johnson.
Office Action dated Aug. 11, 2017 in CN Application No. 2013800234135.
Office Action dated Aug. 21, 2020 in U.S. Appl. No. 12/198,421, by Johnson.
Office Action dated Aug. 22, 2016 in JP Application No. 2014-560097.
Office Action dated Aug. 30, 2021 in JP Application No. 2020114023.
Office Action dated Aug. 31, 2015 in KR Application No. 10-2014-7027734.
Office Action dated Sep. 3, 2018 in CN Application No. 201380052598.2.
Office Action dated Sep. 4, 2015 in EP Application No. 13776685.3.
Office Action dated Sep. 7, 2015 in JP Application No. 2014-560097, translation only.
Office Action dated Sep. 8, 2015 in U.S. Appl. No. 12/198,421 by Johnson.
Office Action dated Sep. 10, 2021 in CN Application No. 201910697285.1 (with English Translation of Search Report).
Office Action dated Sep. 14, 2016 in U.S. Appl. No. 12/198,421, by Johnson.
Office Action dated Sep. 28, 2020 in JP Application No. 2019173287.
Office Action dated Nov. 2, 2018 in U.S. Appl. No. 12/198,421, by Johnson.
Office Action dated Nov. 16, 2021 in CN Application No. 201680075318.3.
Office Action dated Nov. 18, 2016 in CN Application No. 201380023413.5.
Office Action dated Nov. 18, 2016 in U.S. Appl. No. 13/829,951, by Johnson.
Office Action dated Dec. 6, 2013 in U.S. Appl. No. 12/848,991 by Babic.
Office Action dated Dec. 13, 2018 in CN Application No. 2013800234135.
Oh et al., "Ionomer Binders Can Improve Discharge Rate Capability in Lithium-Ion Battery Cathodes," Journal of The Electrochemical Society, vol. 158, No. 2, pp A207-A213 (2011).
Ohta et al., "All-solid-state lithium ion battery using garnet-type oxide and Li3BO3 solid electrolytes fabricated by screen-printing," Journal of Power Sources (2013).
Okumura et al., "All-Solid-State Lithium-Ion Battery Using Li2.2C0.8B0.8B0.2O3 Electrolyte", Solid State Ionic, vol. 288, pp. 248-252 (2016).
Owen, "Rechargeable Lithium Batteries," Chemical Society Reviews, vol. 26, pp. 259-267 (1997).
Peters et al., "Ionic Conductivity and Activation Energy for Oxygen Ion Transport in Superlattices - The Multilayer System CSZ (ZrO2 + CaO) / AI203," Solid State Ionics, vol. 178, Nos. 1-2, pp. 67-76 (2007).
Pham et al., "Synthesis and Characterization of Nanostructured Fast Ionic Conductor Li0.30La0.56TiO3," Chemistry ol Materials, vol. 18, No. 18, pp. 4385-4392 (2006).
Popovici et al., "Sol-gel Preparation and Characterization of Perovskite Lanthanum Lithium Titanate," Journal of Materials Science, vol. 42, pp. 3373-3377 (2007).
Ramzy et al., "Tailor-Made Development of Fast Li Ion Conducting Garnet-Like Solid Electrolytes," Applied Materials & Interfaces, vol. 2, No. 2, pp. 385-390 (2010).
Raskovalov et al., "Structure and transport properties of Li7La3Zr2-0.75xAlxO2 superionic solid electrolytes," Journal of Power Sources (2013).
Rowsell et al., "A new class of materials for lithium-ion batteries: iron(III) borates," Journal of Power Sources, vol. 98-98, pp. 254-257 (2001).
Sakamoto, "Lithium Batteries," Michigan State University (2011).
Sanchez et al., "Chemical Modification of Alkoxide Precursors," Journal of Non-Crystalline Solids, vol. 100, pp. 65-76 (1988).
Scanlon, "Lithium Polymer Battery, Final Report for Dec. 8, 1994-Dec. 30, 2002," Energy Storage and Thermal Sciences Branch, Air Force Research Laboratory (2003).
Shannon et al., "New Li Solid Electrolytes", Electro, vol. 22, No. 7, pp. 783-796 (Jul. 1977).
Singhal et al., "High Temperature Solid Oxide Fuel Cells: Fundamentals, Design and Applications," Elsevier Advanced Technology, 430 pages (2003).
Song et al., "Review of Gel-Type Polymer Electrolytes for Lithium-ion Batteries," Journal of Power Sources, vol. 77, pp. 183-197 (1999).
Stramare et al., "Lithium Lanthanum Titanates: A Review," Chemistry of Materials, vol. 15, pp. 3974-3990 (2003).
Sulaiman, "Fabrication and Characterization of LiN03-AI203 Composite Solid Electrolytes," 2013 3rd International Conference on Chemistry and Chemical Engineering, vol. 38, pp. 1-5 (2012).
Sun et al., "High-Strength All-Solid Lithium Ion Electrodes Based on Li4Ti5012," Journal of Power Sources, vol. 196, pp. 6507-11 (2011).
Tadnaga et al., "Low temperature synthesis of highly ion conductive Li7La3Zr2O12-Li3B03 composites," Electrochemistry Communications (Apr. 3, 2013).
Tan et al., "Fabrication and Characterization of Li7La3Zr2012 Thin Films for Lithium Ion Battery," ECS Solid State Letters, vol. 1, No. 6, pp. 057-060 (2012).
Tan et al., "Garnet-type Li7La3Zr2O12 Electrolyte Prepared by a Solution-Based Technique for Lithium ion battery," Water. Res. Soc. Symp. Proc, vol. 1440, 6 pages (2012).
Fan et al., "Synthesis of Cubic Phase Li7La3Zr2O12 Electrolyte for Solid-State Lithium-Ion Batteries," Electrochemical and Solid-State Letters, vol. 15, No. 3, pp. A37-A39 (2012).
Tan, "Materials for energy storage in Lithium-Ion batteries," Dissertation submitted to the University of Utah (Dec. 2012).
Thangadurai et al., "Investigations on Electrical Conductivity and Chemical Compatibility Between Fast Llithium Ion Conducting Garnet-Life Li6BaLa2Ta2O12 and Lithium Battery Cathodes," Journal of Power Sources, vol. 142, pp. 339-344 (2005).
Vijayakumar et al., "Synthesis of Fine Powders of Li3xLa2/3-xTiO3 Perovskite by a Polymerizable Precursor Method," Chemistry of Materials, vol. 16, No. 14, pp. 2719-2724 (2004).
Wang et al., "Ionic/Electronic Conducting Characteristics of LiFePO4 Cathode Materials," Electrochemical and Solid-State Letters, vol. 10, No. 3, pp. A65-A69 (2007).
West, "Basic Solid State Chemistry," John Wiley & Sons Ltd., Ed. 2, pp. vii-xv, 346-351 (1999).
Wohrle et al., "Sol-Gel Synthesis of the Lithium-Ion Conducting Perovskite La0.57Li0.3TiO3 Effect of Synthesis and Thermal Treatments on the Structure and Conducting Properties," Ionics, vol. 2, pp. 442-445 (1996).
Wolfenstine, "Grain Boundary Conductivity in Crystalline LiTi2(PO4)3," Army Research Laboratory (Apr. 2008).

(56) **References Cited**

OTHER PUBLICATIONS

Written Opinion dated Sep. 22, 2014 in Int'l Application No. PCT/US2013/063161.
Wu et al., "Sol-gel preparation and characterization of Li1.3AI0.3Ti1 7(PO4)3 sintered with flux of LiBO2," Rare Metals, vol. 29, No. 5, p. 515(2010).
Xiong et al., "Effects of Annealing Temperature on Structure and Opt-Electric Properties of Ion-Conducting LLTO Thin Films Prepared by RF Magnetron Sputtering," Journal of Alloys and Compounds, vol. 509, pp. 1910-1914 (2011).
Xu et al., "Structures of Orthoborate Anions and Physical Properties of Their Lithium Salt Nonaqueous Solutions," Journal of The Electrochemical Society, vol. 150, No. 1, pp. E74-E80 (2003).
Xu, "Nonaqueous Liquid Electrolytes for Lithium-Based Rechargeable Batteries," Chemical Reviews, vol. 104, pp. 1303-4417 (2004).
Yang et al., "Ionic to Mixed Ionic/Electronic Conduction Transition of Chemically Lithiated Li0.33La0.56TiO3 at Room Temperature: Lithium-ion-Motion Dependent Electron Hopping," Applied Physics Letters, vol. 89, pp. 1-3 (2006).
Yu et al., "A Stable Thin-Film Lithium Electrolyte: Lithium Phosphorus Oxynitride," J. Electrochem. Soc., vol. 144, No. 2, pp. 524-532 (1997).
Zallen, "The Physics of Amorphous Solids," Wiley-VCH, Ed. 1, pp. ix-xi (1983).
Zhang et al., "Effect of lithium borate addition on the physical and electrochemical properties of the lithium ion conductor Li3.4Si0.4P0.6O4," Solid State Ionics, vol. 231, pp. 109-115 (2013).
Int'l Preliminary Report on Patentability dated Dec. 22, 2014 in Int'l Application No. PCT/US2013/063161.
Int'l Search Report and Written Opinion dated Jan. 6, 2012 in Int'l Application No. PCT/US2011/046289.
Int'l Search Report and Written Opinion dated Mar. 25, 2014 in Int'l Application No. PCT/US2013/063160.
Int'l Search Report and Written Opinion dated Apr. 23, 2014 in Int'l Application No. PCT/US2013/063161.
Int'l Search Report and Written Opinion dated Aug. 15, 2013 in Int'l Application No. PCT/US2013/028672.
Int'l Search Report and Written Opinion dated Aug. 22, 2013 in Int'l Application No. PCT/US2013/028633.
Int'l Search Report and Written Opinion dated Aug. 25, 2020 in Int'l Application No. PCT/US2020/026334.
Int'l Search Report dated Feb. 17, 2017 in Int'l Application No. PCT/US2016/068105 (Partial).
Int'l Search Report dated Apr. 12, 2017 in Int'l Application No. PCT/US2016/068105 (Complete).
Jena et al., "Studies on the Ionic Transport and Structural Investigations of La0.5Li0.5TiO3 Perovskite Synthesized by Wet Chemical Methods and the Effect of Ce, Zr Substitution at Ti site," Journal of Materials Science, vol. 40, pp. 4737-4748 (2005).
Jin et al., "Al-doped Li7La3Zr2O12 synthesized by a polymerized complex method," Journal of Power Sources, vol. 196, pp. 8683-8687 (2011).
Jin et al., "All-Solid-State Rechargeable Lithium Ion Battery Fabrication with Al-Doped Li7La3Zr2O12 Solid Electrolyte," Retrieved from <http://intemational.dep.anl.gov/Postdocs/Symposium/Program/Presentations/32.pdf>, Download date: Oct. 8, 2012, original posting date: unknown, 1 page.
Jin et al., "Bulk solid state rechargeable lithium ion battery fabrication with Al-doped Li7La3Zr2O12 electrolyte and Cu0.1V2O5 cathode," Electrochimica Acta, vol. 89, pp. 407-412 (2013).
Jin, "Processing and characterization of secondary solid-state Li-Ion batteries," Dissertation submitted to the University of Notre Dame, 128 pages (Apr. 2013).
Jinlian et al., "Enhanced high temperature performance of LiMn2O4 coated with Li3BO3 solid electrolyte," Bull. Mater. Sci., vol. 36, No. 4, pp. 687-691 (2013).
Kanamura et al., "Three Dimensionally ordered composite solid materials for all solid-state rechargeable lithium batteries" Journal of Power Sources, 146, pp. 86-89, 2005.
Khatun et al., Impact of Lithium Composition on Structural, Electronic and Optical Properties of Lithium Cobaltite Prepared by Solid-state Reaction Journal of Scientific Research, vol. 6, No. 2, pp. 217-231 (2014).
Kim et al., "Characterization of the Interface Between LiCoO2 and Li7La3Zr2O12 in an All-Solid-State Rechargeable Lithium Battery," Journal of Power Sources, vol. 196, pp. 764-767 (2011).
Kishida et al., "Microstructure of the LiCoO2 (cathode)/La2/3-xLi3xTiO3 (electrolyte) Interface and its Influences on the Electrochemical Properties," Acta Materialia, vol. 55, No. 14, pp. 4713-4722 (2007).
Kitaoka et al., "Preparation of La0.5Li0.5TiO3 Perovskite Thin Films by the Sol-Gel Method," Journal of Materials Science, vol. 32, pp. 2063-2070 (1997).
Kobayashi et al., "All-Solid-State Lithium Secondary Battery with Ceramic/Polymer Composite Electrolyte," Solid State Ionics, vol. 152-153, pp. 137-142 (2002).
Kokal et al., "Sol-gel Synthesis and Lithium Ion Conductivity of Li7La3Zr2O12 with a Garnet-Related Type Structure," Solid State Ionics, vol. 185, pp. 42-46 (2011).
Kotobuki et al., "Fabrication of All-Solid-State lithium battery using novel garnet type electrolyte," ECS Meeting Abstracts (2010).
Kotobuki et al., "Fabrication of Three-Dimensional Battery Using Ceramic Electrolyte with Honeycomb Structure by Sol-Gel Process," Journal of The Electrochemical Society, vol. 157, No. 4, pp. A493-A498 (2010).
Kreiter et al., "Sol-gel Routes for Microporous Zirconia and Titania Membranes," J. Sol-Gel Sci. Technol., vol. 48, pp. 203-211 (2008).
Laughlin et al., "Using Sol-Gel Chemistry to Synthesize a Material with Properties Suited for Chemical Sensing," Journal of Chemical Education, vol. 77, No. 1, pp. 77-78 (2000).
Lee et al., "The Production of LiCoO2 Cathode Thick Films for an All-Solid-State Microbattery," Journal of Ceramic Processing Research, vol. 8, No. 2, pp. 106-109 (2007).
Li et al., "Developments of electrolyte systems for lithium-sulfur batteries: a review," Frontiers in Energy Research, vol. 3, No. 5, pp. 1-12 (2015).
Li et al., "Physical and Electrochemical Characterization of Amorphous Lithium Lanthanum Titanate Solid Electrolyte Fhin-Film Fabricated by e-beam Evaportation," Thin Solid Films, vol. 515, pp. 1886-1892 (2006).
Li et al., "Synthesis and Characterization of Li ion Conducting La2/3-xLi3xTiO3 by a Polymerizable Complex Method," Ceramics International, vol. 33, pp. 1591-1595 (2007).
Liu et al., "Enhanced high temperature performance of LiMn204 coated with Li3B03 solid electrolyte," Bull. Mater. Sci., vol. 36, No. 4, pp. 687-691 (2013).
Ma, Ying, "Ceria-based Nanostructured Materials for Low-Temperature Solid Oxide Fuel Cells," School of Information and Communication Technology, Functional Materials Division, Royal Institute of Technology, 52 pages (2012).
Machida et al., "All-Solid-State Lithium Battery with LiCo0.3Ni0.7O2 Fine Powder as Cathode Materials with an Amorphous Sulfide Electrolyte," Journal of The Electrochemical Society, vol. 149, No. 6, pp. A688-A693 (2002).
Maqueda et al., "Structural, Microstructural and Transport Properties Study of Lanthanum Lithium Titanium Perovskite Thin Films Grown by Pulsed Laser Deposition," Thin Solid Films, vol. 516, pp. 1651-1655 (2008).
Masset et al., "Thermal activated (thermal) battery technology Part II Molten salt electrolytes," Journal of Power Sources, vol. 164, pp. 397-414 (2007).
Mateishina et al., "Solid-State Electrochemical Lithium Cells with Oxide Electrodes and Composite Solid Electrolyte," Russian Journal of Electrochemistry, vol. 43, No. 5, pp. 606-608 (2007).
Meda et al., "Lipon Thin Films Grown by Plasma-Enhanced Metalorganic Chemical Vapor Deposition in a N2-H2-Ar Gas Mixture," Thin Solid Films, vol. 520, pp. 1799-1803 (2012).
Mei et al., "Role of amorphous boundary layer in enhancing ionic conductivity of lithium-lanthanum-titanate electrolyte," Electrochimica Acta, vol. 55, pp. 2958-2963 (2010).
Munshi, "Handbook of Solid State Batteries & Capacitors," World Scientific, Chapters 10-12 (1995).

(56) **References Cited**

OTHER PUBLICATIONS

Murugan et al., "Fast Lithium Ion Conduction in Garnet-Type Li7La3Zr2O12," Angewandte Chemie International Edition, vol. 46, pp. 7778-7781 (2007).
Nagata et al., "All Solid Battery with Phosphate Compounds Made Through Sintering Process," Journal of Power Sources, vol. 174, pp. 832-837 (2007).
Nimisha et al., "Chemical and Microstructural Modifications in LiPON Thin Films Exposed to Atmospheric Humidity," Solid State Ionics, vol. 185, pp. 47-51 (2011).
Office Action and Search Report dated Jan. 20, 2021 in TW Application No. 109111527 (with Brief Summary of Relevanl Portions of Office Action).
Office Action dated Jan. 2, 2015 in U.S. Appl. No. 12/198,421 by Johnson.
Office Action dated Jan. 7, 2013 in U.S. Appl. No. 12/198,421 by Johnson.
Office Action dated Jan. 12, 2022 in U.S. Appl. No. 16/592,562, by Allie.
Office Action dated Jan. 15, 2015 in U.S. Appl. No. 13/829,951 by Johnson.
Office Action dated Jan. 16, 2018 in JP Application No. 2015-535773.
Office Action dated Jan. 17, 2017 in CN Application No. 201380052635.
Office Action dated Jan. 18, 2017 in U.S. Appl. No. 13/829,525, by Johnson.
Zhang et al., "Study on Synthesis and Evolution of Sodium Potassium Niobate Ceramic Powders by an Oxalic Acid-Based Sol-Gel Method," Journal of Sol-Gel Science and Technology, vol. 57, pp. 31-35 (2011).
International Search Report dated May 3, 2022 in International Application No. PCT/US2022/011012.
Office Action dated May 16, 2022 in U.S. Appl. No. 16/838,706, by Johnson.
Office Action dated Jun. 20, 2022 in U.S. Appl. No. 16/918,647, by Johnson.
Obrovac et al, "Reversible Cycling of Crystalline Silicon Powder," Journal of the Electrochemical Society, vol. 154, No. 2, pp. A103-A108 (2007).
Limthongkul et al, "Electrochemically-Driven Solid State Amorphization in Lithium-Silicon Alloys and Implications for Lithium Storage," Acta Materialia, vol. 51, pp. 1103-1113 (2003).
Datta et al, "Silicon and Carbon Based Composite Anodes for Lithium Ion Batteries," Journal of Power Sources, vol. 158, pp. 557-563 (2006).
Read et al, "Characterization of the Lithium/Oxygen Organic Electrolyte Battery," Journal of the Electrochemical Society, vol. 149, No. 9, pp. A1190-A1195 (2002).
Abraham et al, "A Polymer Electrolyte-Based Rechargeable Lithium/Oxygen Battery," Journal of the Electrochemical Society, vol. 143, No. 1, pp. 1-5 (1996).
Miles et al, "Cation Effects on the Electrode Reduction of Molten Nitrates," Journal of the Electrochemical Society, vol. 127, pp. 1761-1766 (1980).
Briant et al, "Ionic Conductivity in Lithium and Lithium-Sodium Beta Alumina," Journal of the Electrochemical Society, vol. 128, No. 9, pp. 1830-1834 (1981).
Wang et al, "Ionic Conductivities and Structure of Lithium Phosporus Oxynitride Glasses," Journal of Non-Crystalline Solids, vol. 183, pp. 297-306 (1995).
Kotobuki et al, "Fabrication of All-Solid-State Lithium Battery with Lithium Metal Anode Using Al2O3-Added Li7La3Zr2O12 Solid Electrolyte," Journal of Power Sources, vol. 196, pp. 7750-7754 (2011).
Kotobuki et al, "Compatibility of Li7La3Zr2O12 Solid Electrolyte to All-Solid-State Battery Using Li Metal Anode," Journal of the Electrochemical Society, vol. 157, No. 10, pp. A1076-A1079 (2010).
Miles, Melvin H., "Lithium Batteries Using Molten Nitrate Electrolytes," Battery Conference on Applications and Advances. The Fourteenth Annual, pp. 39-42 (1999).
Int'l Search Report and Written Opinion dated Mar. 16, 2017 in Int'l Application No. PCT/US2017/014035.
International Preliminary Report on Patentability dated Aug. 2, 2018 in International Application No. PCT/US2017/014035.

* cited by examiner

Fig. 1

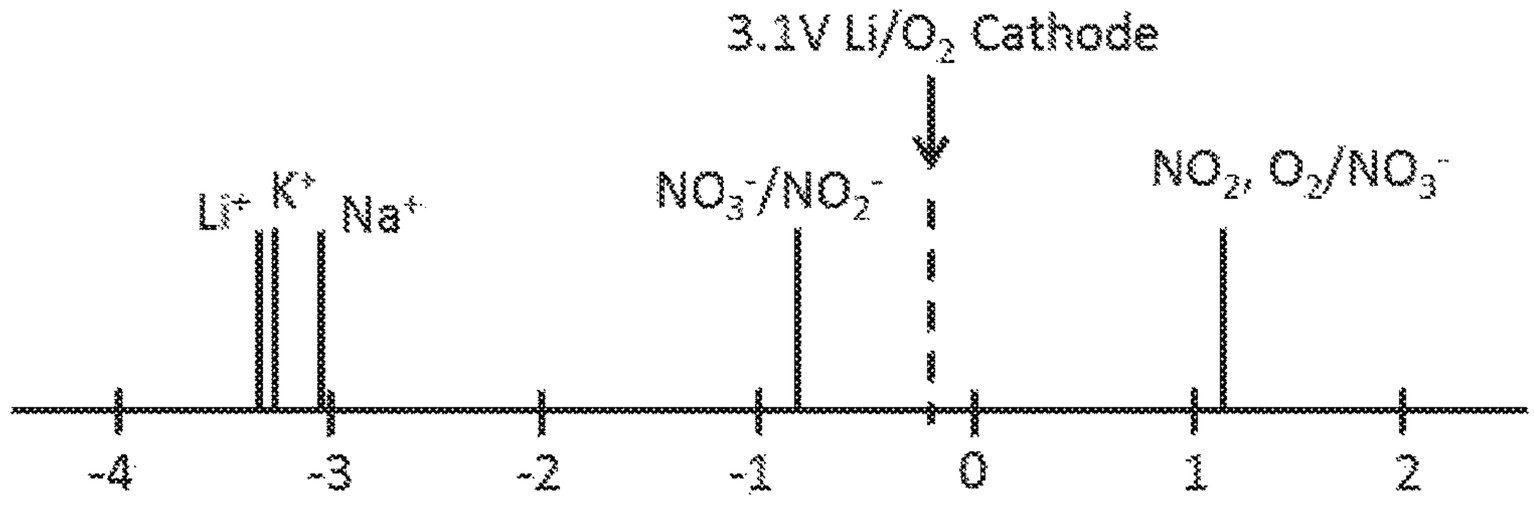

Fig. 2

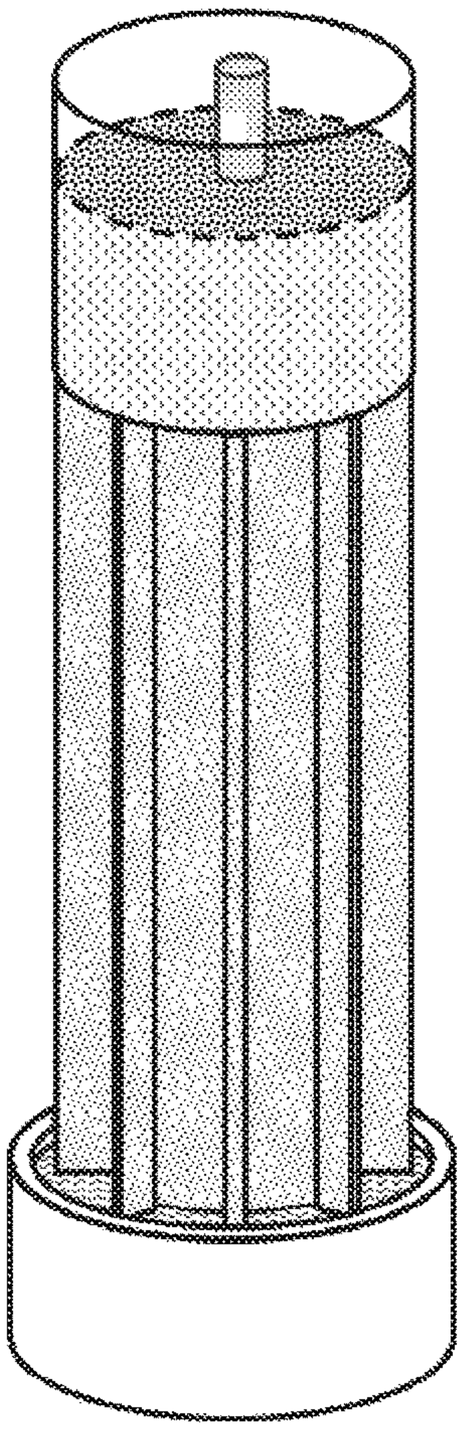

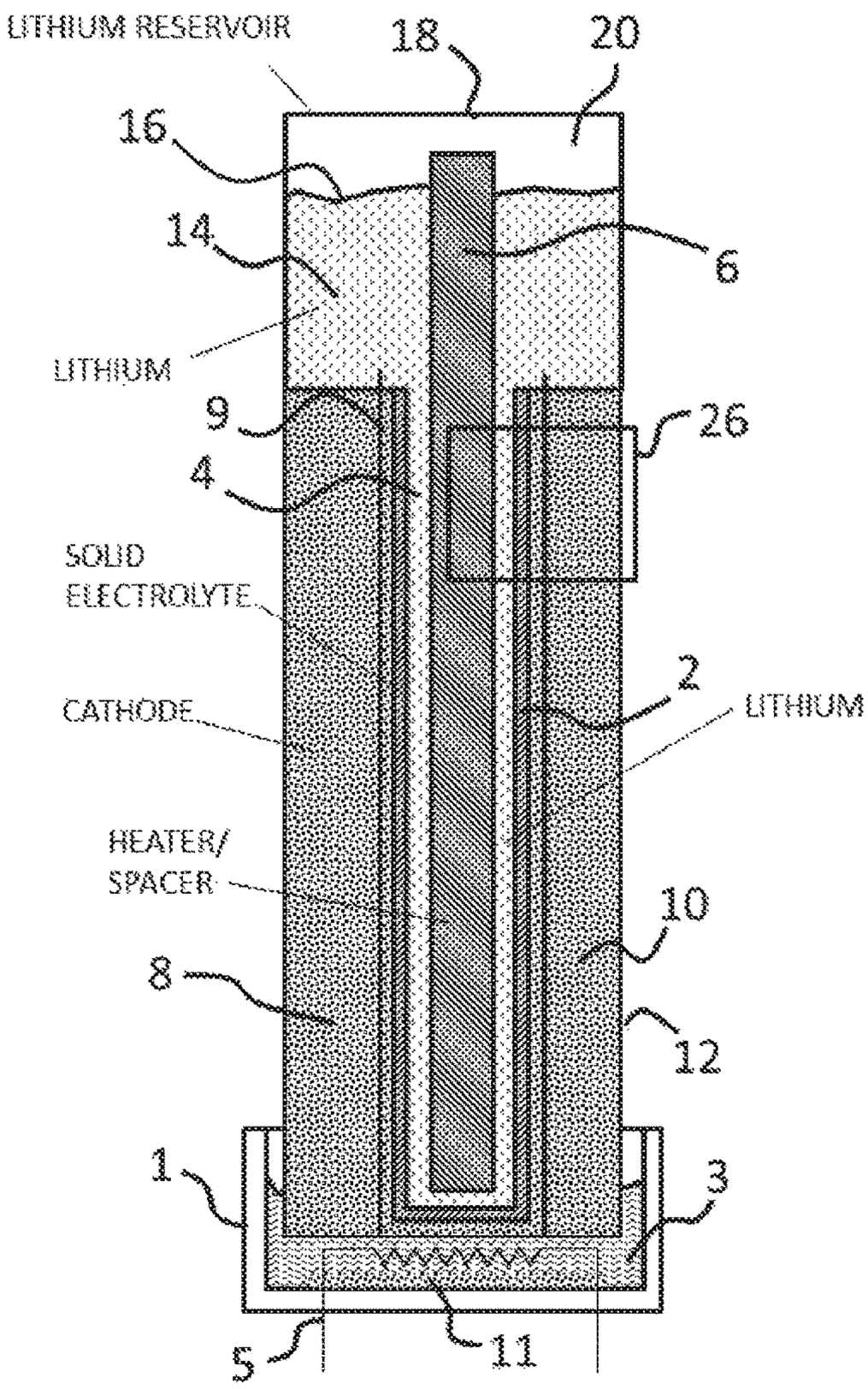
LITHIUM RESERVOIR
18
20
16
14
6
LITHIUM
9
26
4
SOLID ELECTROLYTE
2
CATHODE
LITHIUM
HEATER/ SPACER
10
8
12
1
3
5
11

Fig. 3

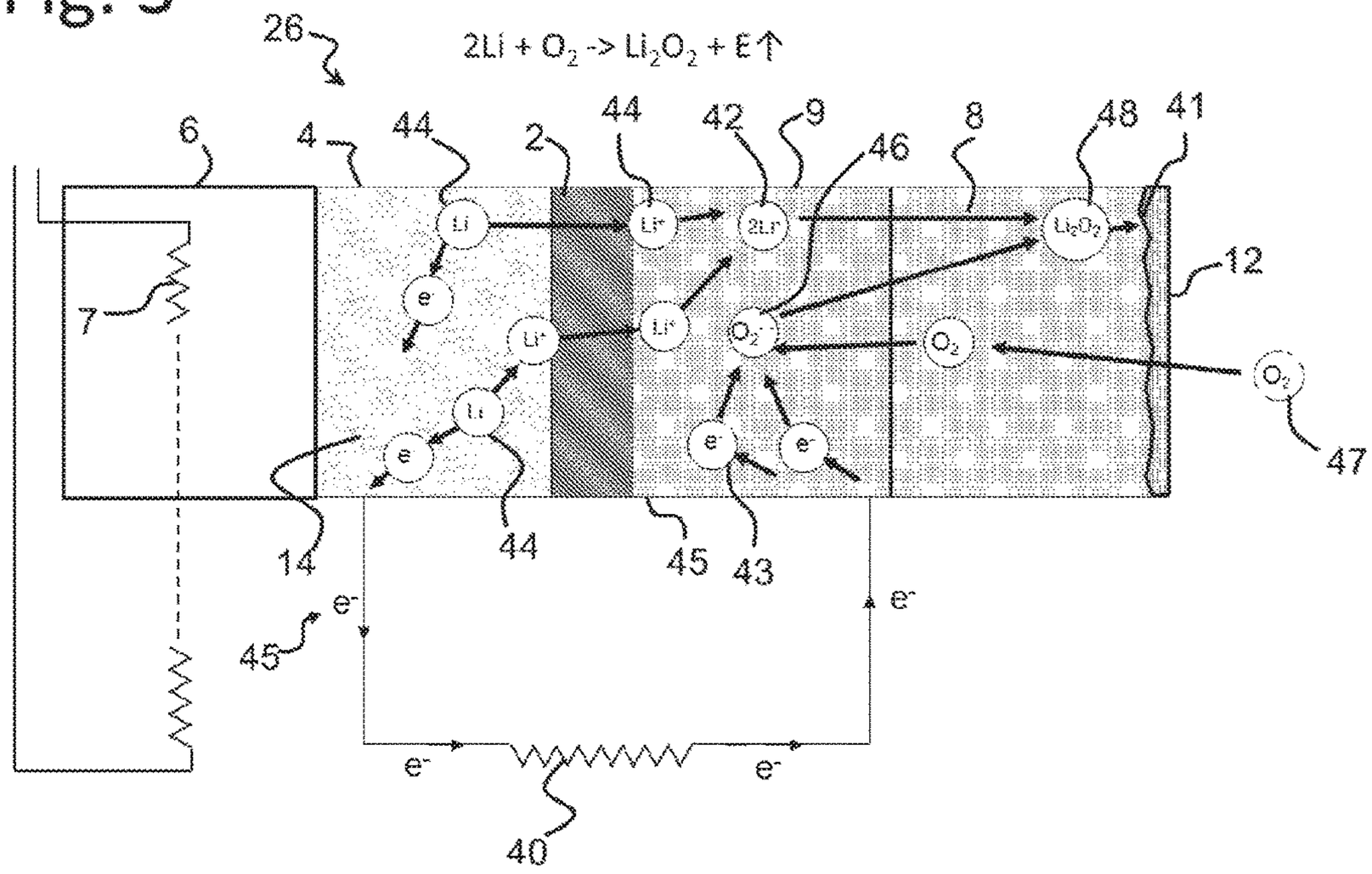

Fig. 4

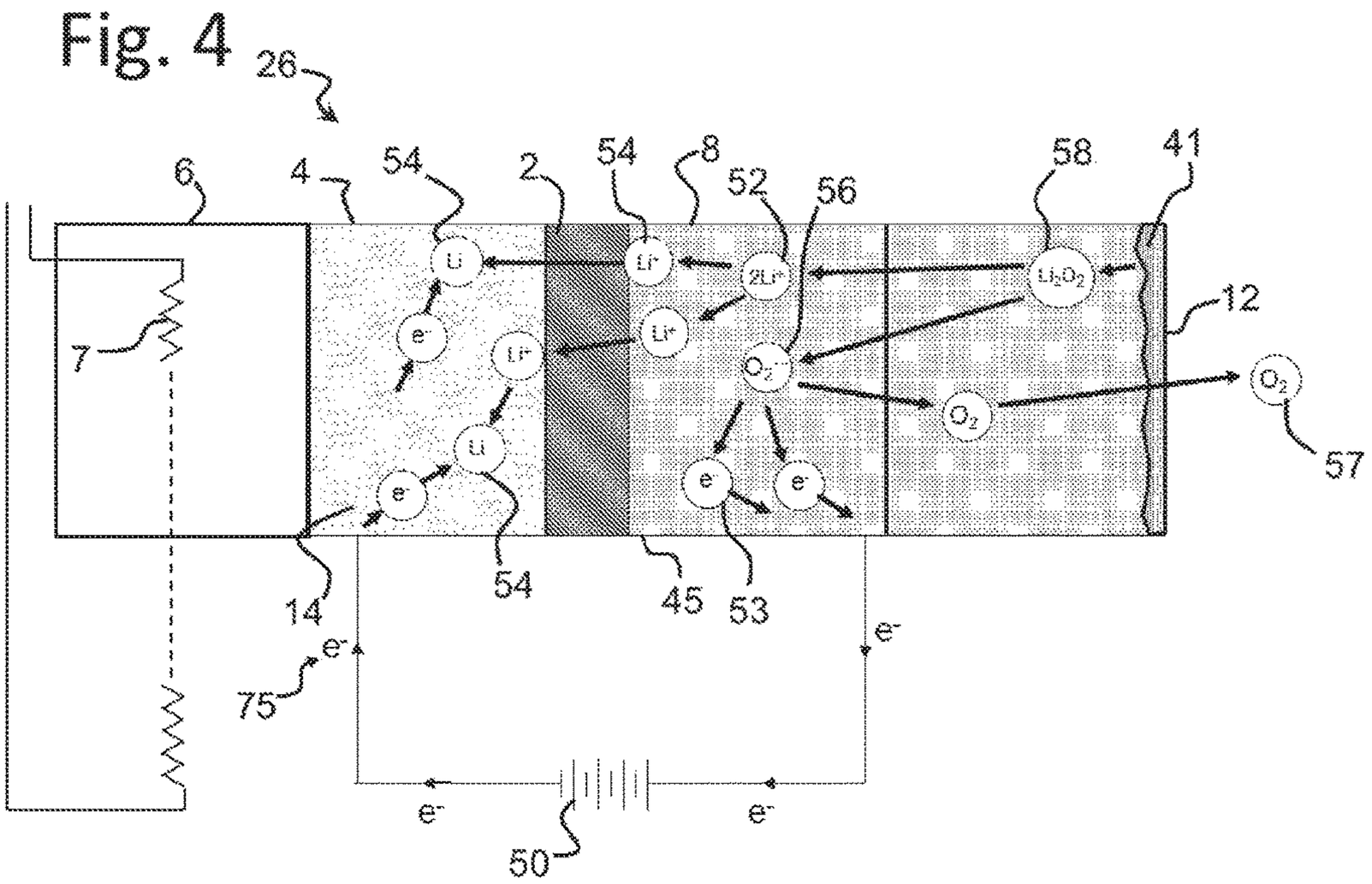
26
6
4
54
2
54
8
52
56
58
41
12
7
Li
e⁻
Li⁺
2Li⁺
Li₂O₂
O₂
57
14
54
45
53
75
50

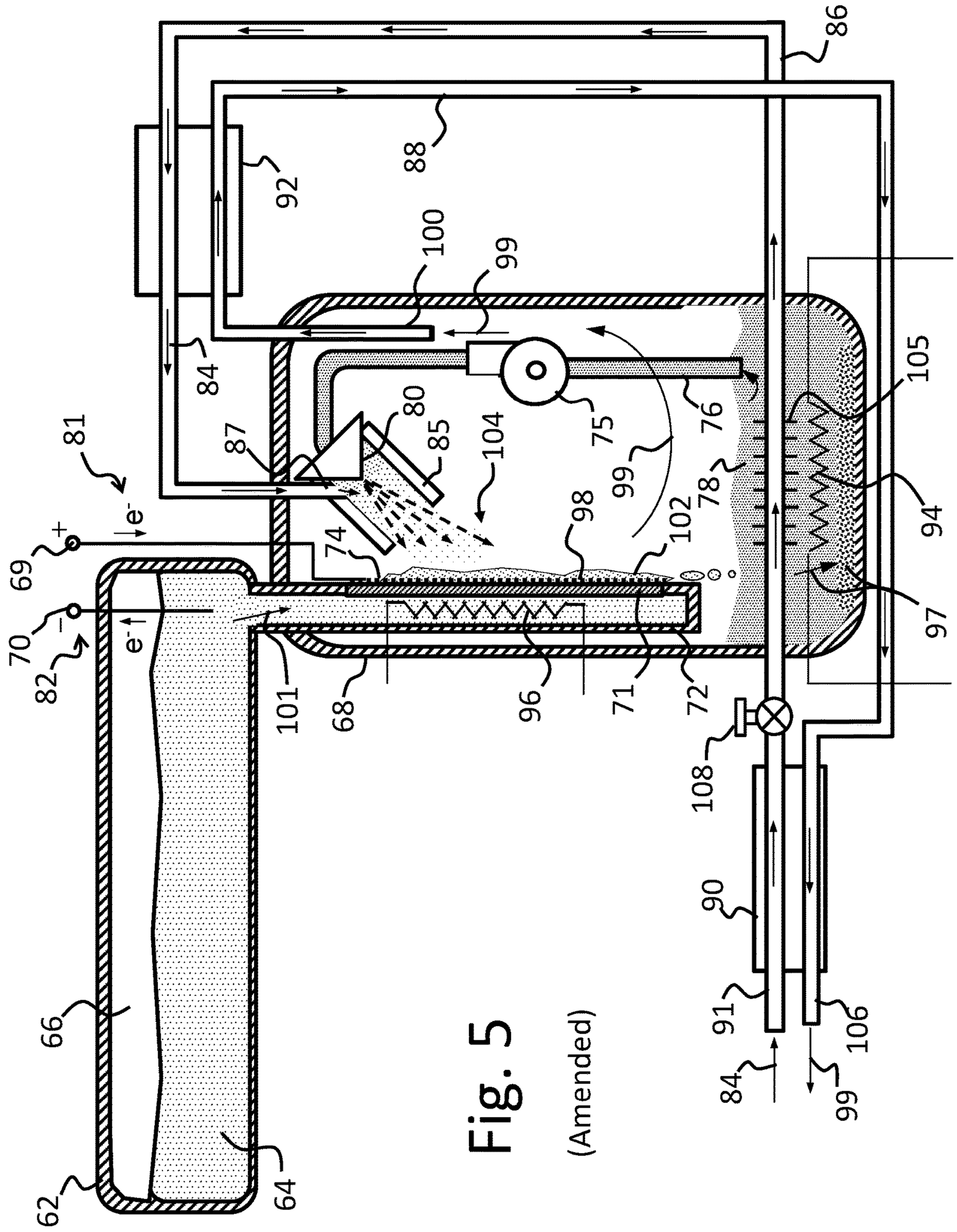

Fig. 5

(Amended)

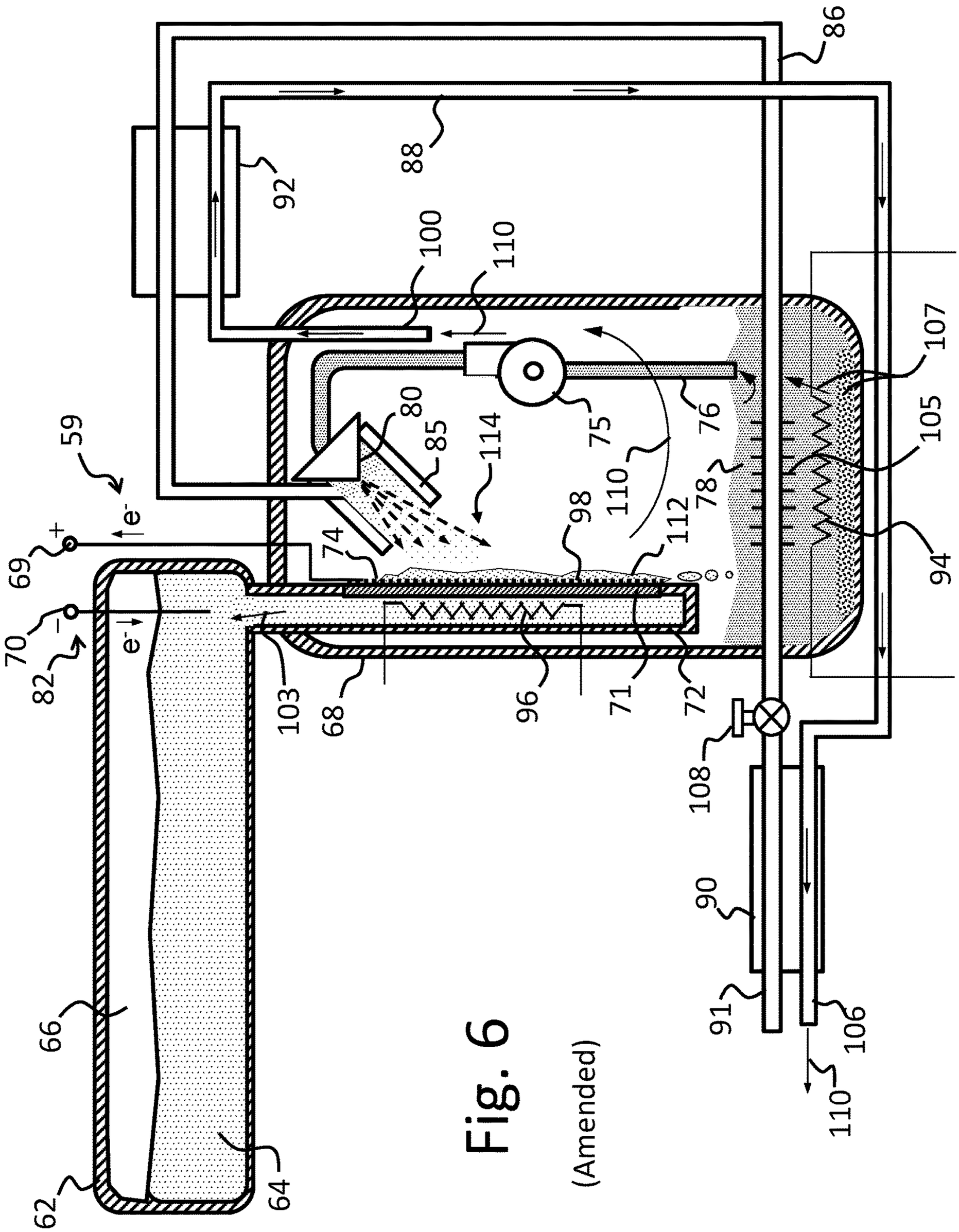

Fig. 6

(Amended)

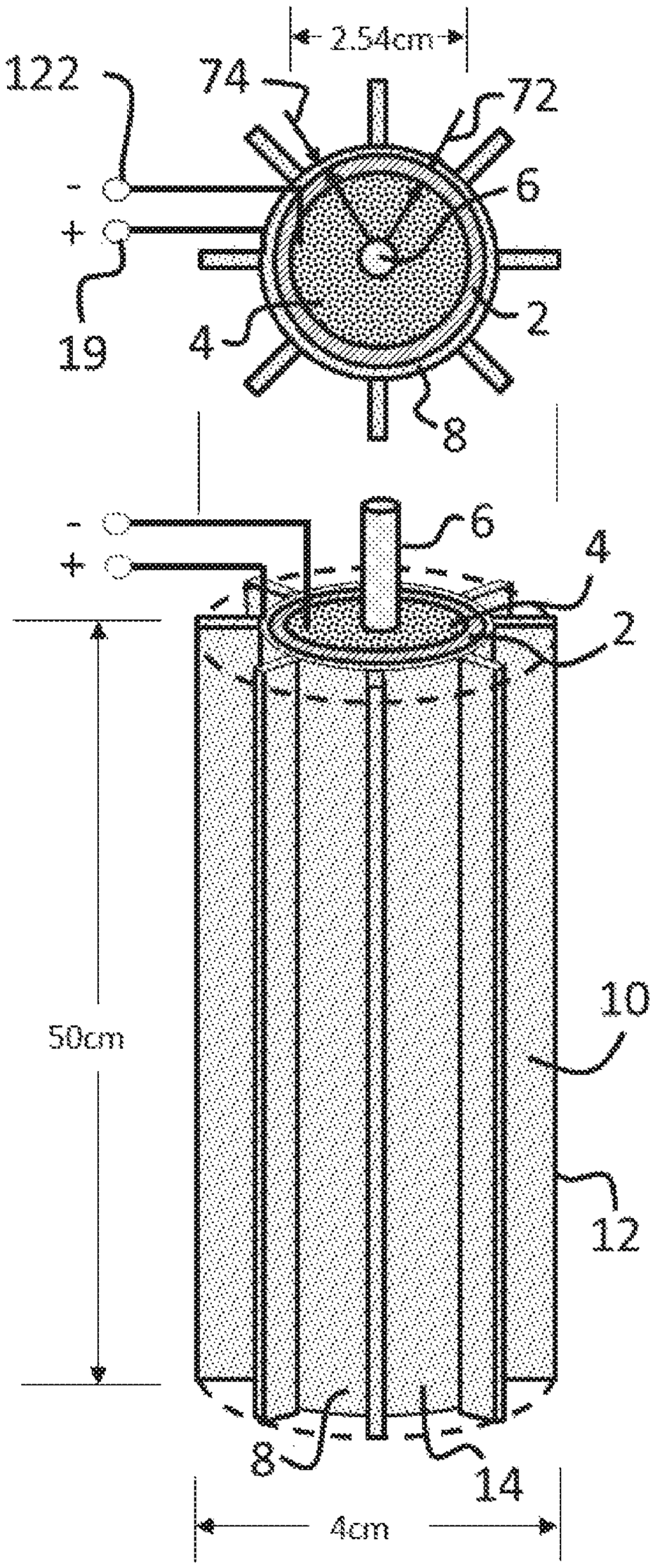

Fig. 7

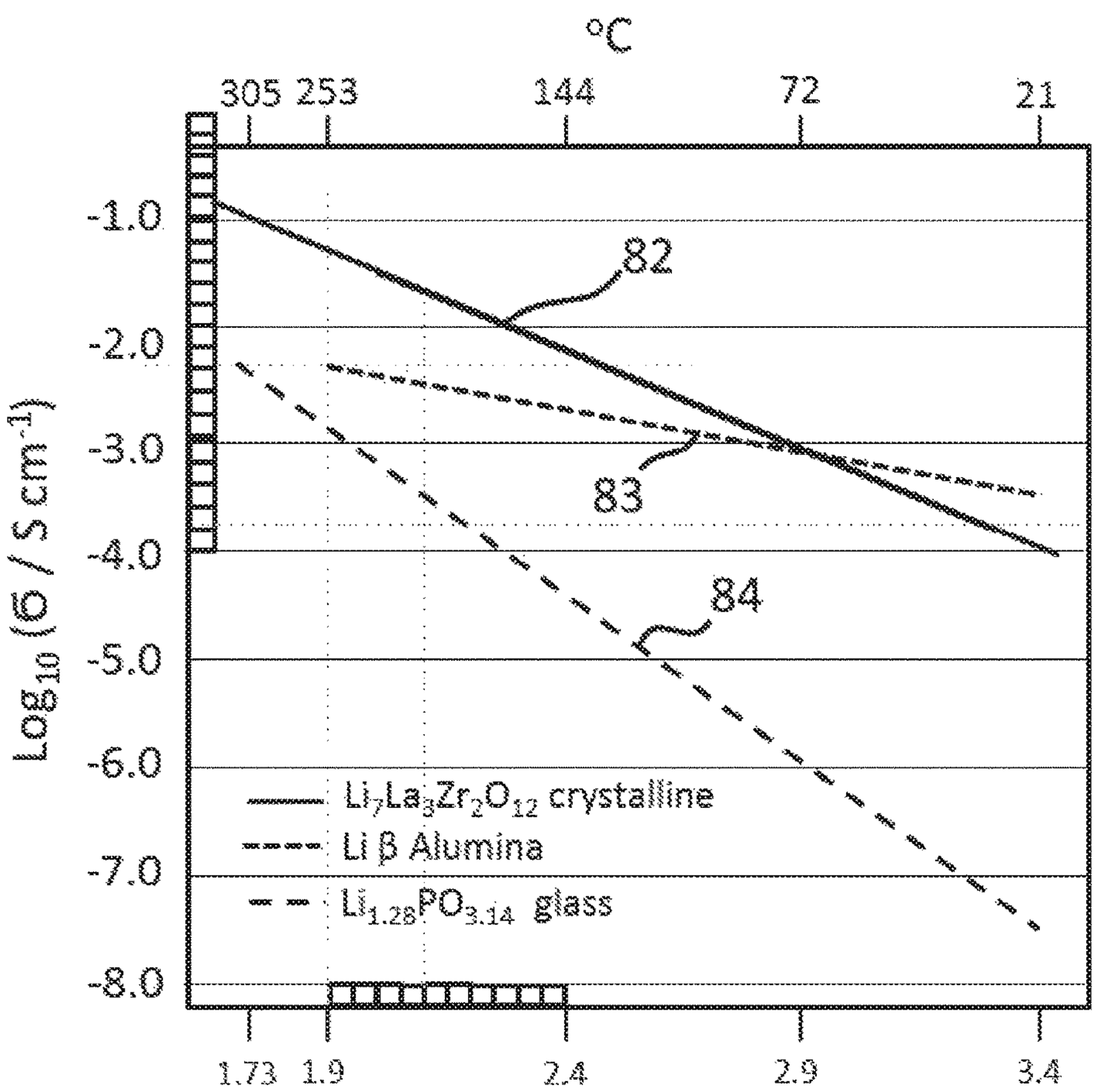
°C
305 253 144 72 21
-1.0
-2.0
-3.0
-4.0
-5.0
-6.0
-7.0
-8.0
82
83
84
Log_{10} (σ / S cm^{-1})
$Li_7La_3Zr_2O_{12}$ crystalline
Li β Alumina
$Li_{1.28}PO_{3.14}$ glass
1.73 1.9 2.4 2.9 3.4
1.6
1000T^{-1} / K^{-1}

Fig. 8

JOHNSON LITHIUM OXYGEN ELECTROCHEMICAL ENGINE

Matter enclosed in heavy brackets [ ] appears in the original patent but forms no part of this reissue specification; matter printed in italics indicates the additions made by reissue; a claim printed with strikethrough indicates that the claim was canceled, disclaimed, or held invalid by a prior post-patent action or proceeding.

CROSS-REFERENCE TO RELATED APPLICATION

This application *is a reissue of U.S. Pat. No. 10,218,044, issued on Feb. 26, 2019 from U.S. application Ser. No. 15/408,991, filed Jan. 18, 2017, which* claims priority to U.S. Provisional Application No. 62/281,875, filed Jan. 22, 2016, the [disclosure] *disclosures* of which [is] *are* herein incorporated by reference *in their entirety*.

BACKGROUND OF THE INVENTION

The need for high performance and reliable energy storage in the modern society is well documented. Lithium batteries represent a very attractive solution to these energy needs due to their superior energy density and high performance. However, available Li-ion storage materials limit the specific energy of conventional Li-ion batteries. While lithium has one of the highest specific capacities of any anode (3861 mAh/g), typical cathode materials such as MnO_2, V_2O_5, $LiCoO_2$ and (CF)n have specific capacities less than 200 mAh/g.

Recently, lithium/oxygen (Li/O_2) or lithium air batteries have been suggested as a means for avoiding the limitations of today's lithium ion cells. In these batteries, lithium metal anodes are used to maximize anode capacity and the cathode capacity of Li air batteries is maximized by not storing the cathode active material in the battery. Instead, ambient O_2 is reduced on a catalytic air electrode to form O_2^{2-}, where it reacts with Li^+ ions conducted from the anode. Aqueous lithium air batteries have been found to suffer from corrosion of the Li anode by water and suffer from less than optimum capacity because of the excess water required for effective operation.

Abraham and Jiang (J. Electrochem. Soc., 1996, 143 (1), 1-5) reported a non-aqueous Li/O_2 battery with an open circuit voltage close to 3 V, an operating voltage of 2.0 to 2.8 V, good coulomb efficiency, and some re-chargeability, but with severe capacity fade, limiting the lifetime to only a few cycles. Further, in non-aqueous cells, the electrolyte has to wet the lithium oxygen reaction product in order for it to be electrolyzed during recharge. It has been found that the limited solubility of the reaction product in available organic electrolytes necessitates the use of excess amounts of electrolyte to adequately wet the extremely high surface area nanoscale discharge deposits produced in the cathode. Thus, the required excess electrolyte significantly decreases high energy density that would otherwise be available in lithium oxygen cells.

Operation of Li/O_2 cells depends on the diffusion of oxygen into the air cathode. Oxygen absorption is a function of the electrolyte's Bunsen coefficient (α), electrolyte conductivity (σ), and viscosity (η). It is known that as the solvent's viscosity increases, there are decreases in lithium reaction capacity and Bunsen coefficients. Additionally, the electrolyte has an even more direct effect on overall cell capacity as the ability to dissolve reaction product is crucial. This problem has persisted in one form or another in known batteries.

Indeed, high rates of capacity fade remain a problem for non-aqueous rechargeable lithium air batteries and have represented a significant barrier to their commercialization. The high fade is attributed primarily to parasitic reactions occurring between the electrolyte and the mossy lithium powder and dendrites formed at the anode-electrolyte interface during cell recharge, as well as the passivation reactions between the electrolyte and the LiO_2 radical which occurs as an intermediate step in reducing Li_2O_2 during recharge.

During recharge, lithium ions are conducted across the electrolyte separator with lithium being plated at the anode. The recharge process can be complicated by the formation of low density lithium dendrites and lithium powder as opposed to a dense lithium metal film. In addition to passivation reactions with the electrolyte, the mossy lithium formed during recharge can be oxidized in the presence of oxygen into mossy lithium oxide. A thick layer of lithium oxide and/or electrolyte passivation reaction product on the anode can increase the impedance of the cell and thereby lower performance. Formation of mossy lithium with cycling can also result in large amounts of lithium being disconnected within the cell and thereby being rendered ineffective.

Lithium dendrites can penetrate the separator, resulting in internal short circuits within the cell. Repeated cycling causes the electrolyte to break down, in addition to reducing the oxygen passivation material coated on the anode surface. This results in the formation of a layer composed of mossy lithium, lithium-oxide and lithium-electrolyte reaction products at the metal anode's surface which drives up cell impedance and consumes the electrolyte, bringing about cell dry out.

Attempts to use active (non lithium metal) anodes to eliminate dendritic lithium plating have not been successful because of the similarities in the structure of the anode and cathode. In such lithium air "ion" batteries, both the anode and cathode contain carbon or another electronic conductor as a medium for providing electronic continuity. Carbon black in the cathode provides electronic continuity and reaction sites for lithium oxide formation. To form an active anode, graphitic carbon is included in the anode for intercalation of lithium and carbon black is included for electronic continuity. Unfortunately, the use of graphite and carbon black in the anode can also provide reaction sites for lithium oxide formation. At a reaction potential of approximately 3 volts relative to the low voltage of lithium intercalation into graphite, oxygen reactions would dominate in the anode as well as in the cathode. Applying existing lithium ion battery construction techniques to lithium oxygen cells would allow oxygen to diffuse throughout all elements of the cell structure. With lithium/oxygen reactions occurring in both the anode and cathode, creation of a voltage potential differential between the two is difficult. An equal oxidation reaction potential would exist within the two electrodes, resulting in no voltage.

As a solution to the problem of dendritic lithium plating and uncontrolled oxygen diffusion, known aqueous and non-aqueous lithium air batteries have included a barrier electrolyte separator, typically a ceramic material, to protect the lithium anode and provide a hard surface onto which lithium can be plated during recharge. However, formation of a reliable, cost effective barrier has been difficult. A lithium air cell employing a protective solid state lithium ion conductive barrier as a separator to protect lithium in a

lithium air cell is described in U.S. Pat. No. 7,691,536 of Johnson. Thin film barriers have limited effectiveness in withstanding the mechanical stress associated with stripping and plating lithium at the anode or the swelling and contraction of the cathode during cycling. Moreover, thick lithium ion conductive ceramic plates, while offering excellent protective barrier properties, are extremely difficult to fabricate, add significant mass to the cell, and are rather expensive to make.

As it relates to the cathode, the dramatic decrease in cell capacity as the discharge rate is increased is attributed to the accumulation of reaction product in the cathode. At high discharge rate, oxygen entering the cathode at its surface does not have an opportunity to diffuse or otherwise transition to reaction sites deeper within the cathode. The discharge reactions occur at the cathode surface, resulting in the formation of a reaction product crust that seals the surface of the cathode and prevents additional oxygen from entering. Starved of oxygen, the discharge process cannot be sustained.

Another significant challenge with lithium air cells has been electrolyte stability within the cathode. The primary discharge product in lithium oxygen cells is Li_2O_2. During recharge, the resulting lithium oxygen radical, LiO_2, an intermediate product which occurs while electrolyzing Li_2O_2, aggressively attacks and decomposes the electrolyte within the cathode, causing it to lose its effectiveness.

High temperature molten salts have been suggested as an alternative to organic electrolytes in non-aqueous lithium-air cells. U.S. Pat. No. 4,803,134 of Sammells describes a high lithium-oxygen secondary cell in which a ceramic oxygen ion conductor is employed. The cell includes a lithium-containing negative electrode in contact with a lithium ion conducting molten salt electrolyte, LiF—LiCl—Li_2O, separated from the positive electrode by the oxygen ion conducting solid electrolyte. The ion conductivity limitations of available solid oxide electrolytes require that such a cell be operated in the 700° C. range or higher in order to have reasonable charge/discharge cycle rates. The geometry of the cell is such that the discharge reaction product accumulates within the molten salt between the anode and the solid oxide electrolyte. The required space is an additional source of impedance within the cell.

TABLE 1

Physical properties of Molten Nitrate Electrolytes

System	Mol %	Melt Temp ° C.	κ (S/cm) @570K	at Mol %
$LiNO_3$—KNO_3	42-58	124	0.687	50.12 mol % $LiNO_3$
$LiNO_3$—$RbNO_3$	30-70	148	0.539	50 mol % $RbNO_3$
$NaNO_3$—$RbNO_3$	44-56	178	0.519	50 mol % $RbNO_3$
$LiNO_3$—$NaNO_3$	56-44	187	0.985	49.96 mol % $NaNO_3$
$NaNO_3$—KNO_3	46-54	222	0.66	50.31 mol % $NaNO_3$
KNO_3—$RbNO_3$	30-70	290	0.394	70 mol % $RbNO_3$

Molten nitrates also offer a viable solution and the physical properties of molten nitrate electrolytes are summarized in Table 1 (taken from Lithium Batteries Using Molten Nitrate Electrolytes by Melvin H. Miles; Research Department (Code 4T4220D); Naval Air Warfare Center Weapons Division; China Luke, Calif. 93555-61000).

The electrochemical oxidation of the molten $LiNO_3$ occurs at about 1.1 V vs. Ag+/Ag or 4.5 V vs. Li+/Li. The electrochemical reduction of $LiNO_3$ occurs at about −0.9V vs. Ag+/Ag, and thus these two reactions define a 2.0V electrochemical stability region for molten $LiNO_3$ at 300° C. and are defined as follows:

$$LiNO_3 \rightarrow Li^+ + NO_2 + \tfrac{1}{2}O_2 + e^- \quad \text{(Equation 1)}$$

$$LiNO_3 + 2e^- \rightarrow LiNO_2 + O^{--} \quad \text{(Equation 2)}$$

This work with molten nitrates was not performed with lithium air cells in mind; however, the effective operating voltage window for the electrolyte is suitable for such an application. As indicated by the reaction potential line in FIG. **1**, applying a recharge voltage of 4.5V referenced to the lithium anode can cause lithium nitrate to decompose to lithium nitrite, releasing oxygen. On the other hand, lithium can reduce $LiNO_3$ to Li_2O and $LiNO_2$. This reaction occurs when the $LiNO_3$ voltage drops below 2.5V relative to lithium. As long as there is dissolved oxygen in the electrolyte, the reaction kinetics will favor the lithium oxygen reactions over $LiNO_3$ reduction. Oxide ions are readily converted to peroxide (O_2^{2-}) and aggressive superoxide (O_2^-) ions in $NaNO_3$ and KNO_3 melts (M. H. Miles et al., J. Electrochem. Soc., 127,1761 (1980)).

A need remains for a lithium air cell which overcomes problems associated with those of the prior art.

BRIEF SUMMARY OF THE INVENTION

A rechargeable lithium air battery comprises a ceramic separator forming an anode chamber, a molten lithium anode contained in the anode chamber, an air cathode, and a non-aqueous electrolyte, wherein the cathode has a temperature gradient comprising a low temperature region and a high temperature region, and wherein the temperature gradient provides a flow system for reaction product produced by the battery.

BRIEF DESCRIPTION OF THE SEVERAL VIEWS OF THE DRAWINGS

The foregoing summary, as well as the following detailed description of the invention, will be better understood when read in conjunction with the appended drawings. For the purpose of illustrating the invention, there are shown in the drawings embodiments which are presently preferred. It should be understood, however, that the invention is not limited to the precise arrangements and instrumentalities shown.

In the drawings:

FIG. **1** is a diagram depicting electrochemical reaction potentials in molten lithium nitrate at 300° C.;

FIG. **2** is a schematic of a battery cell according to one embodiment of the present invention;

FIG. **3** is a schematic of a battery cell according to another embodiment of the present invention in discharge;

FIG. **4** is a schematic of the battery cell of FIG. **3** in recharge;

FIG. **5** is a schematic of a high performance battery cell according to a further embodiment of the invention in discharge;

FIG. **6** is a schematic of a high performance battery cell of FIG. **5** in recharge;

FIG. **7** is a schematic of a battery cell according to a further embodiment of the invention; and

FIG. **8** is an Arrhenius plot showing lithium ion conductivities of several solid ceramic electrolytes.

DETAILED DESCRIPTION OF THE INVENTION

This invention relates generally to energy storage, and more particularly to a lithium air electrochemical cell. For the purposes of this disclosure, the terms lithium air cell, lithium air electrochemical engine and lithium oxygen battery are used interchangeably.

The present invention provides a rechargeable lithium air cell having a high rate of cell charge/discharge with limited capacity fade, high energy density, high power density, and the ability to operate on oxygen from ambient air. As such, it removes significant barriers that have prevented the commercialization of lithium air cells. For example, the formation of mossy lithium powder and dendrites at the anode-electrolyte interface during cell recharge are eliminated by the use of molten lithium supplied as a flow reactant to the anode side of a stable solid state ceramic electrolyte. The battery according to the invention also includes a flow system for removing reaction product from the cathode.

The reactions of lithium with oxygen are as follows:

$$2Li+O_2 \rightarrow Li_2O_2 \quad E_o=3.10\ V$$

$$4Li+O_2 \rightarrow 2Li_2O \quad E_o=2.91V$$

To avoid problems associated with past approaches to lithium air cells, a lithium air cell according to the invention may be operated at a wide range of temperatures in the range of 20° C. to 700° C., which include elevated temperatures, such as the preferred temperatures of about 200° C. to 450° C., more preferably about 200° to about 250° C. The solvent in the electrolyte may be selected based on the preferred operating temperature of the specific battery. Operation at elevated temperature enables faster kinetics for higher power density, thus eliminating a major issue associated with lithium air technology. Further, operation at elevated temperature also allows for the use of high temperature organic electrolytes and inorganic, molten salt electrolyte solutions that have high electrochemical stability, thus avoiding another of the major problems that has plagued conventional approaches to lithium air cells. Selected inorganic molten salts have good solubility of lithium/oxygen reaction products, thus allowing better control of cell kinetics.

The rechargeable air battery according to the invention contains a ceramic separator which forms an anode chamber, a molten lithium anode contained in the anode chamber, an air cathode, and a non-aqueous electrolyte. Each of these components will be described in more detail below.

The cell further comprises a flow system which is provided by a temperature gradient across the cathode. More specifically, the cathode has two temperature regions: a high temperature region (preferably located near the anode, where the reaction takes place) and a low temperature region which is located further away from the anode. As the electrolyte circulates through the cell during discharge, the reaction product produced by the battery migrates from the high temperature region to the low temperature region.

The anode chamber is preferably formed by a sealed ceramic enclosure that is lithium ion conductive and which functions as the separator for the battery. Preferably, the ceramic material is stable in contact with lithium metal and protects the anode from ambient oxygen and moisture. Preferred materials include lithium ion conducting glasses such as lithium beta alumina, lithium phosphate glass, lithium lanthanum zirconium oxide (LLZO), Al_2O_3: $Li_7La_3Zr_2O_{12}$, lithium aluminum germanium phosphate (LAGP), and lithium aluminum titanium phosphate (LATP). In a preferred embodiment, the anode chamber is maintained at about 20° C. to about 200° C., more preferably at about 175° C. to about 200° C., most preferably about 175° C. to about 195° C.

The anode comprises metallic lithium in a molten state; lithium has a melting point of about 180° C. The benefit of the molten lithium anode is that it limits undesirable dendrite growth in the cell.

The non-aqueous electrolyte is chosen for stability in contact with lithium. Thus, a breach in the ceramic enclosure will not result in rapid reactions, particularly because air ingress into the cell will be controlled. Preferred electrolytes include molten inorganic salts, for example, alkali nitrates such as lithium and sodium nitrate, alkali chlorides and bromides such as lithium, potassium and sodium chlorides and bromides, alkali carbonates such as sodium and lithium carbonates, as well as sodium nitrate-potassium nitrate ($NaNO_3$—KNO_3) eutectic mixtures and silane and siloxane-based compounds including, for example, hexamethylcyclotrisiloxane, octamethylcyclotetrasiloxane, decamethylcyclopentasiloxane, and dodecamethylhexatetrasiloxane with or without polyethylene oxide groups.

The inorganic salt, silane, or siloxane in the electrolyte is present in a solvent. The solvent is not limited, and may be selected based on the preferred operating temperature of the battery. A preferred solvent is LiCl—KCl eutectic, which works at a temperature of 350° C. to 450° C. The temperature of the electrolyte may be controlled with a heater and is preferably about 200° C. to 450° C.

The air cathode or positive electrode is porous so that oxygen can penetrate through the pores and form lithium peroxide as the reaction product; electrolyte also flows through the porous cathode. The cathode is preferably formed from a porous ceramic material which is lithium conductive and which is infiltrated or impregnated with a metal nitrate such as silver nitrate or a carbon material such as carbon fibers, carbon black, or carbon foam. Preferred porous ceramic materials include LLZO, LAGP, LATP, and lithium oxyanions such as lithium carbonate; most preferred is LLZO. In another preferred embodiment, the cathode contains a carbon material, a heat resistance polymer binder such as polyimide, and a metal oxide catalyst. An exemplary cathode material of this type contains about 60% by weight vapor grown carbon fibers, about 30% polyimide binder, and about 10% manganese dioxide. The cathode may also be constructed of electrically conductive sintered metal oxide powder, sintered metal nitride, carbon, or sintered silicon carbide.

As a preferred example, porous lithium lanthanum zirconium oxide (LLZO) ceramic substrates are prepared by pressing 10-15 grams of LLZO powder into a disc at 1000 psi. The disc is densified by placing in a furnace at 1000° C. for a period of 1 hour. The disc is then impregnated with a metal nitrate such as silver nitrate to form the cathode.

A thermodynamic process is employed to remove and supply electrolyte to cathode reaction sites. In its basic configuration, a temperature gradient is maintained across the structure of the cathode wetted by the electrolyte. The active charge/discharge reaction region of the cell forms the higher temperature region of the gradient. As a result of the temperature gradient, during discharge, reaction product accumulated within the electrolyte at the higher temperature region migrates to the lower temperature region where it

precipitates/solidifies. The configuration of the cell is such that reaction product can accumulate within the lower temperature region physically away from the higher temperature reaction region of the cell. Accumulation of reaction product in the lower temperature region prevents it from significantly affecting the charge/discharge cell kinetics occurring in the higher temperature cathode reaction region. Ultimately, the cooled and settled reaction product will become re-dissolved in the electrolyte. This flow system is a key attribute of the inventive batteries.

In an alternative embodiment, the cell contains a pump to circulate the electrolyte across the temperature gradient. Such a cell contains a molten or another appropriate electrolyte reservoir and a temperature control system for controlling the relative temperatures of the cathode and the reservoir. Further, a heating element is employed for electrolyte temperature control. The pump system cycles electrolyte between the cathode and the electrolyte reservoir, which are adjacent to and in fluid communication with each other. Operation is such that during discharge, the cathode is maintained at a temperature that is elevated above that of the electrolyte reservoir. Reaction product dissolved in the electrolyte at high temperature in the cathode is carried to the electrolyte reservoir where it precipitates due to the lower temperature therein. In contrast, during charge, heat is supplied to the reservoir to maintain solubility of reaction product into the electrolyte. During charge, the electrolyte carries dissolved reaction product from the reservoir to the cathode, where it is electrolyzed. Oxygen is released and lithium ions are conducted through the ceramic separator such that lithium metal is plated at the anode. Electrolyte depleted of reaction product circulates back to the reservoir where it dissolves and carries more reaction product to the cathode as the charge process continues. The configuration is such that the reaction product is temporarily stored as a solid in the electrolyte reservoir as opposed to the cathode. Operation in this manner enables the cathode to be maintained in an optimum configuration for maximum charge and discharge performance.

FIG. **2** is a schematic drawing of a molten lithium electrochemical cell according to an embodiment of the invention. The cell is cylindrical in shape with fins running lengthwise along the cylinder and radiating outward away from the core of the cell. The basic structure is supported by hollow solid electrolyte cylinder (anode chamber) **2** which extends the length of the cell and functions as the cell separator. Molten lithium metal **14** is contained within reservoir **18** at the top of the cell and inside annular cavity **4** such that molten lithium is free to flow down from reservoir **18** into annular cavity **4**. The top level of the molten anode **16** is not expected to totally fill the headspace **20** of the cell. Electrical heater element **6** runs the length of the cell and is positioned to maintain the lithium in a molten state. Heater **6** is part of the core structure that forms annular cavity **4** between the heater and the inner wall of the solid electrolyte **2** where molten lithium **14** is contained. Lithium **14** serves as the anode of the cell. Fined cathode cylinder **8** is positioned over the outer surface of electrolyte cylinder **2**. The core of the fin is shown by **9**. Cathode **8** is a porous structure containing liquid electrolyte which, due to its finned structure, is configured to have a wicking effect to maintain distribution of electrolyte therein. The reaction in the cell occurs at the interface where the cathode touches the separator, which is the hotter (high temperature) region of the cathode. The reaction product will not settle in this hot portion of the cathode, but rather on the colder side of the cathode (low temperature region). This allows for deeper cathode access. The cell preferably operates at 250° C. to 700° C. such that the eutectic salt mixture or other electrolyte is maintained in a molten state. Fins **10** extend into the surrounding air to facilitate heat transfer to the air such that heat supplied to the core induces a temperature gradient radially outward that is maintained between tips **12** of the fins **10** and the molten lithium at the core of the cell.

Dissolved reaction product **11** generated during discharge will preferentially precipitate in the lower temperature regions of the fins as opposed to the warmer core region. Molten electrolyte reservoir **1** contains excess electrolyte **3** and electrolyte that has been displaced by reaction product as it is produced and deposited within fins **10**. Reservoir **1** may be maintained at a temperature that is lower than the core of the cell such that the reaction product preferentially precipitates therein as well. The temperature of the reservoir is controlled by heater element **5**. During recharge, reaction product re-dissolves into the molten salt electrolyte to maintain concentration equilibrium as product is electrolyzed and lithium is re-plated at the anode. Heater **5** is used during recharge to heat the electrolyte to redissolve reaction product. The heat source for core **6** of the cell is not shown but would maintain temperature for operation during both charge and discharge.

Reservoir **18** supplies lithium **14** to annular cavity **4** so that the cavity does not become depleted as the lithium is consumed during discharge. Similarly, as lithium is reduced into the annular section during recharge, lithium is resupplied and accumulated in the reservoir.

FIGS. **3** and **4** show expanded views of radial plane cross section **26** of the cell in FIG. **2** and illustrate the operation of the cell. These Figs. show heater/spacer **6** including heater element **7**, finned cathode **8**, annular lithium cavity **4**, solid electrolyte cylinder **2** and molten lithium anode **14**. Referring to FIG. **3**, oxygen **47** dissolves into the molten salt electrolyte from the cell's environment. During discharge, lithium **44** is oxidized and conducted through electrolyte separator **2** into the molten salt contained within cathode **8**, giving rise to electric current flow **45** through load **40** to cathode **8**. The electrons **43** oxidize molecular oxygen that is dissolved in the molten salt electrolyte, producing oxygen ions **46** to complete the reaction, with the resulting reaction product being either lithium peroxide (Li_2O_2 as $2Li^+$ and O_2^{--}) and/or lithium oxide (Li_2O as $2Li^+$ and O^{--}) ions suspended in the molten salt electrolyte solution. The two lithium ions **42** are anticipated to be individually dispersed within the electrolyte. The illustration is not intended to convey a diatomic pair bonded to each other. When the molten salt becomes saturated with reaction product, lithium peroxide **48** and/or lithium oxide begins to precipitate out of solution.

Heater element **7** located in the center region of the cell maintains the lithium anode and the electrolyte salt contained in the cathode in a molten state. Because of its location and because of the loss of heat from the cathode fins to the air surrounding the cell, a decreasing temperature exists between the core of the cell **6** and fin tips **12**. The molar equilibrium of dissolved lithium/oxygen reaction product in the molten salt will be lower at the lower temperature fin tips **12** than at the high temperature cathode material **45** that is closest to the core of the cell. As such, reaction product **48** will tend to precipitate out of solution in the region of fin tips **12**, resulting in a buildup of reaction product **41** in that location. Although reaction kinetics will favor the high temperature region, creation of reaction product in high temperature region **14** will cause over saturation and precipitation of reaction product in lower

temperature fin tip region **12**. Migration to fin tips **12** will occur because the molar concentration of reaction product in the salt is continuous between the two regions. The salt level will naturally be uniformly distributed, limited only by mass transport rate across the concentration gradients of the dissolved product within the molten salt. Further production of reaction products in the solution in the higher temperature regions will cause precipitation of reaction product in the lower temperature region since the increase would cause over saturation in the low temperature region.

Having the reaction product accumulate in the fin tip regions of the cell is important because precipitation in this region has only very limited adverse impacts on operation of the cell. The invention thus avoids over accumulation of reaction product in the active region of the cell which could cause a reduction of ionic conductivity and could block access and diffusion of oxygen to reaction sites.

FIG. **4** depicts recharge operation of the cell. For recharge, power source **50** is connected in the circuit in place of the load. Dissolved lithium/oxygen reaction product **52**, **54**, **56** is electrolyzed as electrons **53** are stripped by the power source and coupled to the anode side of the cell. During the process, molecular oxygen **57** is released to the environment and lithium ions **54** are conducted through the solid state separator **2** to the anode side of the cell where electrons **53** reduce it to lithium metal.

As reaction product **58** is consumed from the molten salt electrolyte solution, its molar concentration level in the electrolyte eutectic tends lower, thus allowing additional reaction product precipitant **41** to dissolve into the electrolyte. The re-dissolved reaction product naturally migrates toward the core region of the cell due to the concentration gradient created as reaction product in the core region is removed by the recharge process. Continuous dissolving of reaction product **41** maintains a molar equilibrium concentration level of the reaction product in the electrolyte in fin tip region **12** until all of discharge reaction product **41** is re-dissolved and electrolyzed, whereby the cell will be fully charged.

FIG. **5** is a schematic diagram of a high performance lithium oxygen or lithium air cell according to a further embodiment of the invention. Lithium reservoir **62** contains molten lithium **64** at a preferred temperature of 350° C. A portion **72** of lithium reservoir **62** extends into **[**reactor**]** *reaction* chamber *and molten salt electrolyte reservoir* **68** where separator **71** interfaces with the contents of *reaction* chamber *and molten salt electrolyte reservoir* **68**. Reservoir **62** optionally includes ullage pressurized gas **66** to ensure flow of molten lithium into contact with solid state electrolyte separator **71**. Reservoir **62** maintains the supply **101** of lithium to separator **71** as the cell is discharged. Separator **71** is a solid lithium ion conductive material and may be lithium beta alumina or lithium lanthanum zirconium oxide (LLZO). It is preferably a solid ceramic and/or a glass electrolyte. Cathode **98** and embedded current collector **74** are coupled to the surface of separator **71** on the external side of reservoir **62**. Cathode **98** includes lithium/oxygen reaction sites for charge and discharge of the cell. Current collector **74** is connected to positive terminal **69** which allows electrons **81** to travel. Power is applied to terminals **82**. **[**Reactor**]** *Reaction* chamber *and molten salt electrolyte reservoir* **68** contains molten *salt* electrolyte **78**. Pump **75** supplies *molten salt* electrolyte **[**solution**]** **78** through supply tube **76** to nozzle **80**. Nozzle **80**, tube **85** and port **87** comprise a jet pump whereby fluid supplied by pump **75** creates a low pressure region that draws air **84** into port **87** such that it flows through conduit **86** to port **87**. The fluid injection process creates a turbulent mixture region of air and molten electrolyte. It produces a washing effect as the resulting spray **104** exits the jet pump and impinges on cathode **98**. This process creates an electrochemical potential between the lithium inside reservoir **62** on one side of electrolyte **71** (electrode terminal **70**) and the oxygen dissolved and dispersed within electrolyte/air mixture washing through cathode **98** on the other side.

Operation of the cell is such that molten salt electrolyte **102** washing through cathode **98** dissolves lithium-air reaction products produced therein as the cell is discharged. Oxygen depleted air **99** exits the reactor chamber through port **100**. Air **84** enters the cell at port **91** and passes through heat exchanger **90**, heat exchanger **105** and heat exchanger **92** prior to entering reaction chamber *and molten salt electrolyte reservoir* **68**. The flow rate can be controlled by valve **108**. The heat exchangers preheat air **84** to a level such that it enters nozzle **87** near the temperature of molten salt electrolyte **78** exiting nozzle **80**. Air entering the reaction chamber *and molten salt electrolyte reservoir* **68** is heated within heat exchangers **90** and **92** by oxygen depleted air **99** exiting the reaction chamber through conduit **88**. Air passing through heat exchanger **105** inside **[**reactor**]** *reaction chamber and molten salt electrolyte reservoir* **68** is heated by molten electrolyte salt **78**. Extraction of heat from electrolyte **78** in the electrolyte reservoir maintains its temperature below the temperature of the electrolyte **102** that is washing through cathode **98**. Electric heater **96** is thermally coupled to separator **71** and supplies energy as needed to maintain the temperature of cathode **98** above the temperature the reservoir electrolyte **78** that is thermally coupled to heat exchanger **105**. The effect of the thus maintained temperature difference is that electrolyte **102** washing through cathode **98** is raised to a higher temperature than electrolyte **78** that is in the reservoir. Continuous flow of electrolyte continuously dissolves and washes away reaction product being produced in cathode **98**. On the other hand, when the electrolyte leaves cathode **98** and is cooled by heat exchanger **105** in the reservoir, its saturation limit for dissolved reaction product decreases, which causes a portion of the reaction product to precipitate, **97**. The electric heater **94** is used to control the temperature of the electrolyte. The discharge process continues as pump **75** resupplies electrolyte **78**, now depleted of reaction product, to nozzle **80** where it entrains more air and carries it to cathode **98**, is reheated, and dissolves more reaction product as it occurs from lithium air reactions ongoing therein.

FIG. **6** illustrates operation of the cell under recharge conditions. Power is supplied to heater **94** to increase the solubility level of reaction product **107** in electrolyte **78**. The dissolving of reaction product **107** in electrolyte **78** increases with temperature. Pump **75** pumps electrolyte **78** containing dissolved reaction product to nozzle **80** whereby it is sprayed **114** onto cathode **98**. Power is applied to terminals **82** to electrolyze lithium/air reaction product in cathode **98**. With the extraction of electrons **59** by a positive voltage applied to terminal **69** relative to terminal **70**, reaction product is electrolyzed with oxygen **110** being released to escape **[**reactor**]** *reaction* chamber *and molten salt electrolyte reservoir* **68** via port **100**. It exits the cell through port **[78]** *106* after passing through heat exchanger **92** and **90** to preheat incoming air. During the recharge process, lithium ions are conducted through solid electrolyte separator **71** into reservoir **62** where it is reduced to lithium by electron flow via terminal **70**. The recharge process continuously electrolyzes dissolved reaction product from molten salt in cathode **98** as reaction product depleted electrolyte **112**

returns to *reaction chamber and molten salt electrolyte* reservoir **[78]** *68*, dissolves more reaction product, **107**, and is pumped back to cathode **98**. Molten lithium is re-supplied to reservoir **62** as indicated by arrow **103**. Under recharge condition, valve **108** may optionally be closed since air intake into the reaction chamber is not needed.

In an exemplary cell shown in FIG. **7**, solid electrolyte cylinder **2** with terminals **122** and **19** has an inner diameter of 2.54 cm and length of 50 cm. The volume of lithium would be 0.253 L ($\pi(2.54(D)/2)^2$*50 cm(L)=253.35 cm^3). The electrochemical potential for the lithium/oxygen reaction is 3.14V. Assuming an under load operating output voltage of 2.5V to allow for internal impedances, the energy capacity can be determined considering the Amp-Hour capacity of lithium being 3,860 Ah/kg (2,084 Ah/ltr). At an output voltage of 2.5V, the energy available from the cell would be 9650 Wh/kg (5210 Wh/ltr). Given the 0.253 L lithium volume in the example, the cell could supply 1.3 kWh of energy.

In a cell operating at 300° C. with $NaNO_3$—KNO_3 molten salt eutectic electrolyte, the conductivity of the electrolyte is 0.66 S/cm. Similarly, the conductivity of the solid electrolyte containment cylinder **2** at 300° C. is 0.1 S/cm as shown in FIG. **7**. Assuming that the thickness **74** in FIG. **7** of the porous cathode **8** on the surface of the solid cylinder electrolyte **2** is 0.2 cm and that the thickness **72** of the solid electrolyte is 0.1 mm, the area specific resistance of the solid electrolyte plus the liquid can be calculated as 0.403 Ohm-cm^2 (1/(0.66 S/cm)*0.2 cm+1/(0.1 S/cm)*0.01 cm). Given the 0.7 Volt allowance for internal IR loss, the net output current under load would be 1.73 A assuming other polarization losses are negligible. In such a case, the area specific power of the cell would be 4.34 Watts. This example cell has a surface area of 399 cm^2(π*2.54*50), therefor its power output capability would be 1.73 kW.

FIG. **8** is an Arrhenius plot showing the conductivity of several solid state ionic conductive materials that would be suitable for use as the electrolyte cylinder **2**. Impedance line **83** is for lithium beta alumina (data from J. L. Briant, J. Electrochem. Soc.: Electrochemical Science And Technology; 1834 (1981)) and line **84** is for lithium phosphate glass (data from B. Wang, Journal of Non-Crystalline Solids, Volume 183, Issue 3, 2; 297-306 (1995). Conductivity values **82** for aluminum oxide doped lithium lanthanum zirconium oxide (Al_2O_3:$Li_7La_3Zr_2O_{12}$) are from M Kotobuki, et. al.; Journal of Power Sources 196 7750-7754 (2011)).

Sintered LLZO electrolyte had been demonstrated to be stable with lithium in all solid state batteries. (See T. Yoshida, et. al.; Journal of The Electrochemical Society, 157-10, A1076-A1079 (2010)). The cyclic voltammogram of the Li/LLZO/Li cell showed that the dissolution and deposition reactions of lithium occurred reversibly without any reaction with LLZO. This indicates that a Li metal anode can be employed in contact with LLZO electrolyte.

In an exemplary embodiment, a 1 kWh battery is designed to operate at a discharge rate of 1 C, i.e. battery totally discharged in 1 hour. Lithium has a specific energy of 11,580 Wh/kg. If the mass of the oxygen is included, the net energy density is 5,200 Wh/kg. For a 1 kWh battery, 86 g of lithium would be needed. Lithium has a discharge current capacity of 3.86 Ah/g. At a discharge rate of 1 C, the required discharge current would be 332 A (86 g*3.86 Ah/g/1 hr). In this example, the area of the separator may be defined as 100 cm^2 and the solid separator as LLZO or other suitable substitute thereof. In this example the use of a 100 cm^2 separator results in a net current density of 3.32 A/cm^2. As indicated in FIG. **8**, the lithium ion conductivity, σ, of LLZO is approximately 0.1 S/cm. A separator made of this material and at a thickness, t, of 100 um would have an impedance of 0.1 Ohm-cm^2, ($1/\sigma$*t). The output current supplied at 1 C would have a maximum drop in voltage of 0.4V relative to the cell's open circuit voltage. The primary reaction product of the cell is Li_2O_2. The amount of air flow required to sustain a 1 C discharge rate can be determined from the required oxygen flow.

The atomic mass of lithium is 6.9 g/mole. The primary discharge reaction for the cell is $2Li+O_2>Li_2O_2$, 1 mole of oxygen is required for per mole of lithium. The number of moles of lithium in the reaction is 12.46, (86 g/6.9 g/mole). Therefore, 6.23 moles or 199.4 grams (6.23 moles *32 grams/mole) of oxygen are required to balance the reaction. Air is 23% oxygen by mass so that the total amount of air needed for the reaction is 866 g, (199.4 g O_2/(0.23 g O_2/gAir). For the 1 C discharge, the air mass flow rate is 866 g/hr or 0.24 g/sec. The density of air is 0.00123 g/cm^3. This gives a volumetric flow rate of 195 cm^3/sec.

It will be appreciated by those skilled in the art that changes could be made to the embodiments described above without departing from the broad inventive concept thereof. It is understood, therefore, that this invention is not limited to the particular embodiments disclosed, but it is intended to cover modifications within the spirit and scope of the present invention as defined by the appended claims.

We claim:

1. A rechargeable lithium air battery comprising a ceramic separator forming an anode chamber, a molten lithium anode contained in the anode chamber, an air cathode, a non-aqueous electrolyte, and an electrolyte reservoir adjacent to the cathode, wherein the cathode has a temperature gradient comprising a low temperature region and a high temperature region, and wherein the temperature gradient provides a flow system for reaction product produced by the battery.

2. The battery according to claim **1**, further comprising a pump and a temperature control system.

3. The battery according to claim **2**, wherein the pump controls movement of the electrolyte between the cathode and the electrolyte reservoir.

4. The battery according to claim **2**, wherein the temperature control system controls temperatures of the cathode and the electrolyte reservoir.

5. The battery according to claim **1**, wherein during discharge the reaction product moves from the high temperature region of the cathode to the low temperature region of the cathode.

6. The battery according to claim **1**, wherein the electrolyte comprises a molten inorganic salt.

7. The battery according to claim **1**, wherein the electrolyte comprises a silane or siloxane compound.

8. The battery according to claim **1**, wherein the cathode comprises a porous ceramic material.

9. The battery according to claim **8**, wherein the cathode is impregnated with a metal nitride or a carbon material.

10. The battery according to claim **1**, wherein the cathode comprises an electrically conductive sintered metal oxide, metal nitride, carbon, or silicon carbide.

11. The battery according to claim **1**, wherein the cathode comprises carbon, a polymer binder, and a metal oxide.

12. The battery according to claim **8**, wherein the porous ceramic material comprises lithium lanthanum zirconium oxide.

13. The battery according to claim **1**, where the anode chamber is maintained at about 20° C. to 200° C.

14. The battery according to claim **1**, wherein the ceramic separator comprises a lithium ion conducting glass.

15. The battery according to claim **14**, wherein the lithium ion conducting glass is selected from lithium beta alumina, lithium phosphate glass, lithium lanthanum zirconium oxide, Al_2O_3:$Li_7La_3Zr_2O_{12}$, lithium aluminum germanium phosphate, and lithium aluminum titanium phosphate.

16. The battery according to claim **1**, wherein the battery has an operating temperature of about 200° C. to about 450° C.

17. A rechargeable lithium air battery comprising a ceramic separator forming an anode chamber, a molten lithium anode and a heater contained in the anode chamber, an air cathode, and a non-aqueous electrolyte, wherein the cathode has a temperature gradient comprising a low temperature region and a high temperature region, and wherein the temperature gradient provides a flow system for reaction product produced by the battery.

18. A rechargeable lithium air battery comprising a ceramic separator forming an anode chamber, a molten lithium anode contained in the anode chamber, an air cathode, and a non-aqueous electrolyte, wherein the cathode has a temperature gradient comprising a low temperature region and a high temperature region, the temperature gradient provides a flow system for reaction product produced by the battery, wherein the cathode comprises a core adjacent to the ceramic separator and at least one fin extending radially outward from the core, and wherein the core is the high temperature region of the cathode and the at least one fin is the low temperature region of the cathode.

19. A rechargeable lithium air battery comprising a ceramic separator forming an anode chamber, a molten lithium anode contained in the anode chamber, an air cathode, a non-aqueous electrolyte, an electrolyte reservoir adjacent to the cathode, a pump and a temperature control system, wherein the temperature control system controls temperatures of the cathode and the electrolyte reservoir, the temperature of the electrolyte reservoir is about 200° C. to about 450° C., the cathode has a temperature gradient comprising a low temperature region and a high temperature region, and wherein the temperature gradient provides a flow system for reaction product produced by the battery.

20. A rechargeable lithium air battery comprising a lithium reservoir, a reaction chamber, an air cathode, a temperature control system, and an electrolyte reservoir adjacent to the air cathode, wherein the lithium reservoir includes a ceramic separator and the electrolyte reservoir contains an inorganic non-aqueous electrolyte, the ceramic separator extends into the reaction chamber whereby lithium flows into the reaction chamber from the lithium reservoir and contacts the ceramic separator in the reaction chamber, the ceramic separator couples lithium to the inorganic non-aqueous electrolyte supplied from the electrolyte reservoir, and the inorganic non-aqueous electrolyte couples the reaction chamber to the electrolyte reservoir and carries reaction product therebetween whereby reaction product within the reaction chamber is removed.

21. The battery according to claim 20, wherein the temperature control system controls temperatures of the cathode and the electrolyte reservoir.

22. The battery according to claim 20, wherein the cathode comprises a core adjacent to the ceramic separator and at least one fin extending radially outward from the core.

23. The battery according to claim 22, and wherein the core is a high temperature region of the cathode and the at least one fin is a low temperature region of the cathode.

24. The battery according to claim 20, wherein the electrolyte comprises a molten inorganic salt.

25. The battery according to clam 20, wherein the electrolyte comprises a silane or siloxane compound.

26. The battery according to claim 20, wherein the cathode comprises a ceramic material.

27. The battery according to claim 20, wherein the cathode is impregnated with a metal nitride or a carbon material.

28. The battery according to claim 20, wherein the cathode comprises an electrically conductive sintered metal oxide, metal nitride, carbon, or silicon carbide.

29. The battery according to claim 20, wherein the cathode comprises carbon, a polymer binder, and a metal oxide.

30. The battery according to claim 26, wherein the ceramic material comprises lithium lanthanum zirconium oxide.

31. The battery according to claim 20, where the anode chamber is maintained at about 20° C. to 200° C.

32. The battery according to claim 20, wherein the ceramic separator comprises a lithium ion conducting glass.

33. The battery according to claim 32, wherein the lithium ion conducting glass is selected from lithium beta alumina, lithium phosphate glass, lithium lanthanum zirconium oxide, Al_2O_3:$Li_7La_3Zr_2O_{12}$, lithium aluminum germanium phosphate, and lithium aluminum titanium phosphate.

34. The battery according to claim 20, wherein the battery has an operating temperature of about 200° C. to about 450° C.

35. A rechargeable lithium air battery comprising:
a supply of air flow,
an air cathode,
a heat exchanger for transferring heat to air flowing to the air cathode from air leaving the air cathode,
a pump for supplying air to the air cathode,
a temperature control system,
a lithium ion conductive solid ceramic electrolyte
a lithium reservoir,
an inorganic electrolyte reservoir,
a molten lithium anode contained in the lithium reservoir, and
an inorganic electrolyte contained within the inorganic electrolyte reservoir,
wherein lithium flows to the lithium anode from the lithium reservoir during charge and from the lithium anode to the lithium reservoir during recharge, the solid ceramic electrolyte conducts lithium ions from the lithium reservoir to the inorganic electrolyte for reaction with oxygen supplied by air flow to the air cathode, and wherein lithium oxygen reaction product is accumulated within the electrolyte reservoir.

36. The battery according to clam 35, wherein the lithium oxygen reaction product has at least limited solubility in the inorganic salt electrolyte.

37. A rechargeable lithium air battery comprising:
a supply of air flow,
a heat exchanger,
a pump,
a cathode,
a temperature control system,
a reaction chamber,
a lithium reservoir,
a molten salt electrolyte reservoir,
a molten lithium anode contained in the lithium reservoir, and

a molten inorganic salt electrolyte contained within the molten salt electrolyte reservoir,

wherein lithium is supplied to the reaction chamber from the lithium reservoir, molten inorganic salt is supplied to the reaction chamber from the molten salt electrolyte reservoir and air is supplied to the reaction chamber by the heat exchanger, the heat exchanger transfers heat from oxygen-depleted air leaving the cathode to ambient air flowing to the cathode, and wherein lithium oxygen reaction product accumulates within the molten salt electrolyte reservoir.

38. The battery according to clam 37, wherein the reaction chamber surrounds an air cathode and a solid ceramic lithium ion conductive electrolyte, wherein the solid ceramic lithium ion conductive electrolyte is coupled between the lithium reservoir and the molten inorganic salt electrolyte, isolating lithium from the molten inorganic salt electrolyte, interfacing lithium to the molten salt electrolyte or cathode, and conducting lithium ions from the lithium reservoir to the molten salt electrolyte for reaction with oxygen supplied to the cathode with air flow from the heat exchanger.

39. A rechargeable lithium air battery comprising:

a supply of oxygen flow,

a ceramic lithium ion conductive electrolyte,

a pump,

a lithium reservoir,

an inorganic electrolyte reservoir,

a molten lithium anode,

a cathode, and

an inorganic electrolyte contained within the electrolyte reservoir,

wherein the ceramic electrolyte is coupled between the lithium anode and the cathode, lithium is supplied to the anode from the lithium reservoir, oxygen is supplied to the cathode, and lithium ions are conducted by the ceramic electrolyte to the cathode, whereby lithium reacts with oxygen at the cathode, the pump circulates the electrolyte between the cathode and the reservoir, and the electrolyte washes reaction product from the cathode during discharge and supplies reaction product to the cathode during recharge.

40. A rechargeable lithium air battery comprising:

a supply of oxygen flow,

a cathode,

a ceramic lithium ion conductive electrolyte,

a heat exchanger for transferring heat to air flowing to the cathode from air leaving the cathode,

a lithium reservoir,

an inorganic electrolyte reservoir,

a molten lithium anode,

a pump for supplying air to the cathode, and

an inorganic electrolyte contained within the electrolyte reservoir,

wherein the ceramic electrolyte is coupled between the lithium anode and the cathode, lithium is supplied to the anode from the lithium reservoir, oxygen is supplied to cathode with air supplied by the pump, and lithium ions are conducted by the ceramic electrolyte to the cathode, whereby lithium reacts with oxygen at the cathode, and wherein lithium oxygen reaction product accumulates within the inorganic electrolyte reservoir.

41. A rechargeable lithium air battery comprising:

a supply of air flow,

an air cathode,

an electrolyte pump,

a temperature control system,

a lithium ion conductive solid ceramic electrolyte

a lithium reservoir,

a molten salt electrolyte reservoir,

a molten lithium anode contained in the lithium reservoir, and

a molten inorganic salt electrolyte contained within the molten salt electrolyte reservoir,

wherein the solid ceramic electrolyte conducts lithium ions from the lithium reservoir to the molten inorganic salt electrolyte for reaction with oxygen supplied by air flow to the cathode, and the electrolyte pump promotes electrolyte flow to contact the cathode and to remove and carry lithium oxygen reaction product to the electrolyte reservoir.

* * * * *